AD-A061 256 DAEDALEAN ASSOCIATES INC WOODBINE MD F/G 13/8
RESEARCH OF CONTROLLED CAVITATION EROSION TECHNIQUES FOR UNDERW--ETC(U)
JUN 78 J PARKER, A P THIRUVENGADAM N00014-74-C-0213
UNCLASSIFIED DAI-JP-7435-001-TR NL

1 OF 1
AD
A061 256

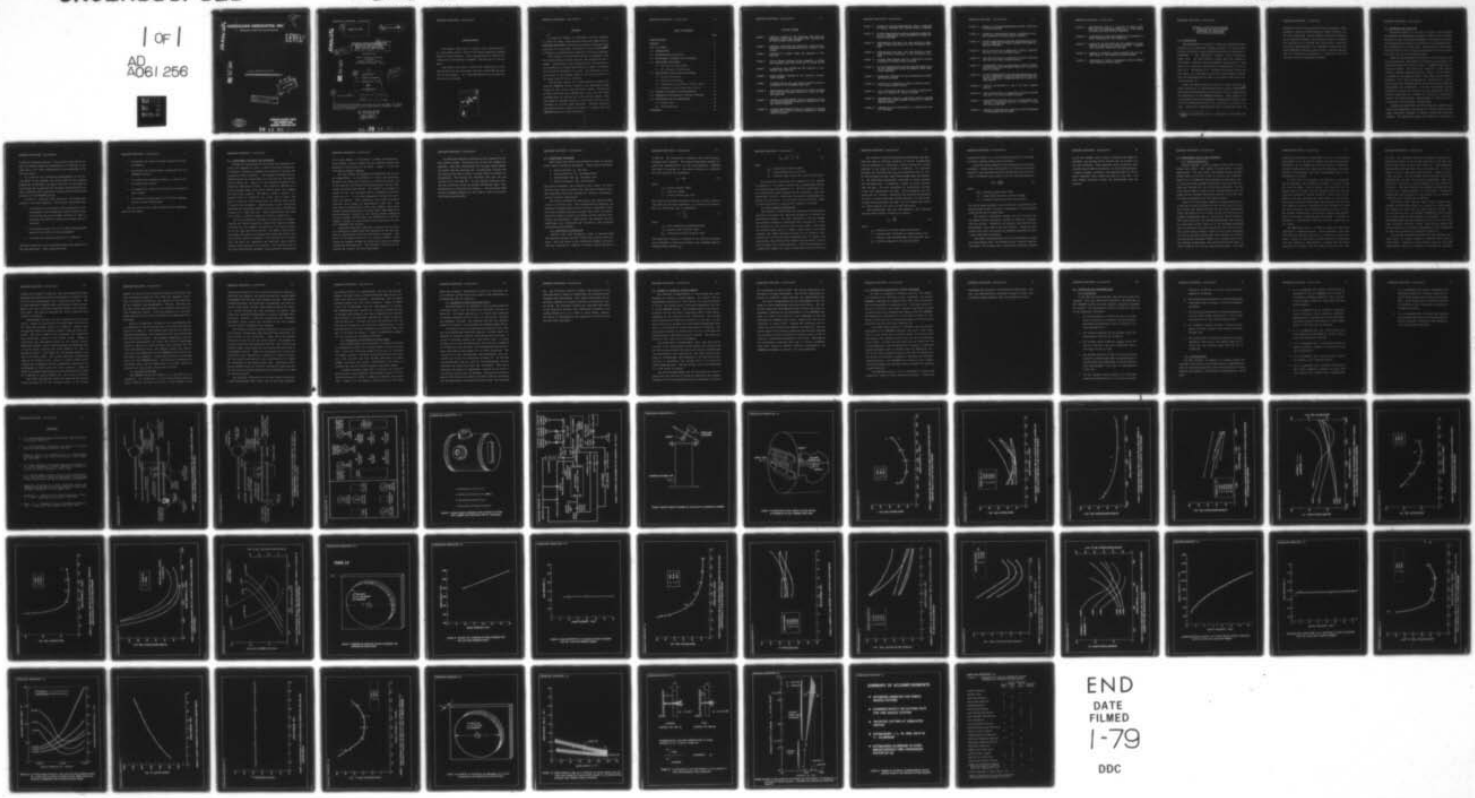

END
DATE
FILMED
1-79
DDC

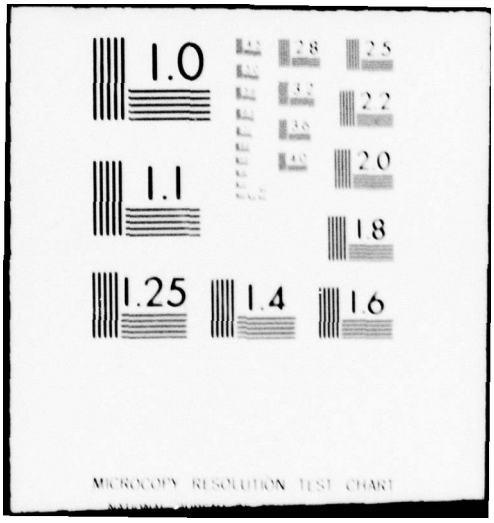
1.0
1.1
1.25
1.4
1.6
2.8
2.5
2.2
2.0
1.8
MICROCOPY RESOLUTION TEST CHART

AD A061256

(2)

SC

DAEDALEAN ASSOCIATES, INC.

ENGINEERING, DESIGN AND ANALYSIS SERVICES

LEVEL II

DDC FILE COPY

Contract N00014-74-C-0213 New

SPRINGLAKE RESEARCH CENTER
15110 FREDERICK ROAD
WOODBINE, MARYLAND 21797

78 11 03 021

DAEDALEAN ASSOCIATES, Incorporated

(15) NØØØ14-74-C-Ø213

(9) TECHNICAL REPORT,

(6) TECHNICAL REPORT ON THE RESEARCH OF CONTROLLED CAVITATION EROSION TECHNIQUES FOR UNDERWATER STEEL CUTTING APPLICATIONS

(12) 79 p.

Prepared for:

Office of Naval Research
Code 485
800 N. Quincy Street
Arlington, Virginia 22217

by

(10) James Parker,
A. P. Thiruvengadam,
A. A. Hochrein, Jr.
and
Frank Graham

(14) DAI-JP-7435-ØØ1-TR

The views and conclusions contained in this document are those of the authors and they do not constitute a standard, specification or regulation.

DAI TECHNICAL REPORT
NO. JP-7435-001-TR

(11) June 1978

ACKNOWLEDGMENTS

The authors would like to express their appreciation to Lt. Christensen and Dr. Silva of the Ocean Technology Program, Office of Naval Research. Their sponsorship and technical assistance has been helpful throughout the duration of the program.

The authors also wish to extend their appreciation to Mr. William Boyd for his assistance with data gathering and analysis in the program. Dr. Thiruvengadam was the principal director of the program.

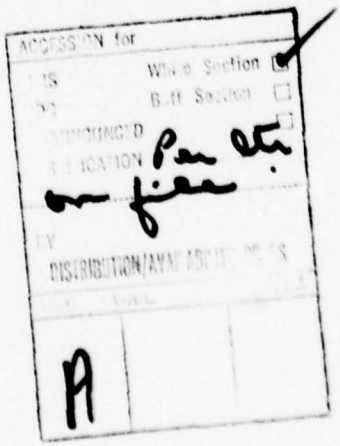

ABSTRACT

A technical advance in underwater cutting equipment is needed for many ocean oriented industrial applications. DAEDALEAN ASSOCIATES, Incorporated engineers investigated the potential of a controlled cavitation erosion (CONCAVER™) technique as an advancement of underwater cutting technology.

The intensity of cavitation erosion is dependent upon the nozzle design, distance, velocity and application environment. Efforts have been concentrated on optimization of the parameters of design and distance in order to maximize the associated intensity of erosion. The intensity of erosion varies as the twelfth power of the nozzle velocity in the range from 750 fps to 1250 fps.

The specific energy for cutting medium strength rock with the CONCAVER system surpasses the comparable energy ratings of the rotary tool and water cannon. Utilization of these abilities has enabled DAI to cut 1/2 inch thick aluminum plate at the rate of 1-1/16 inch per minute. Having advanced aluminum cutting to this point, DAI is on the threshold of cutting steel underwater. Further laboratory experimentation is required in order to characterize the CONCAVER system for field operation.

TABLE OF CONTENTS

LIST OF FIGURES

TECHNICAL REPORT ON THE RESEARCH OF CONTROLLED CAVITATION EROSION TECHNIQUES FOR UNDERWATER STEEL CUTTING APPLICATIONS

1.0 INTRODUCTION

The phenomenon of cavitation erosion has exhibited unique potential as an underwater cutting technique. In the past cavitation erosion has caused rapid deterioration of high speed hydrodynamic systems. Hydrofoils, rudders, marine propellers, pumps, valves and other similar systems have been damaged by the energy released as cavitation bubbles collapse (1,2*). Many years of research have been devoted to minimization of the effect of the phenomenon (3,4). Although cavitation erosion has been viewed as a detriment in the past; when properly controlled, the phenomenon may be used to accomplish tasks with beneficial results (5).

Under the sponsorship of the Office of Naval Research, the basic research for a controlled cavitation erosion (CONCAVER™) system has been developed for underwater cutting to demonstrate the feasibility of the CONCAVER technique. Upon completion of a successful laboratory feasibility demonstration, efforts were directed toward maximization of the intensity of cavitation erosion. Laboratory investigations have concentrated upon the

---

* Numbers in parentheses refer to references at the end of this report.

parameters which directly govern nozzle performance. These parameters consist of nozzle distance, nozzle velocity, nozzle loss coefficient, nozzle diameter and nozzle geometry. As the program continued, the obtained values of intensity and cutting rate in aluminum have consistently increased. Continued experimentation and equipment fabrication have moved CONCAVER technology progressively toward the ultimate goal of cutting steel underwater at comparable rates with existing state-of-technology equipment.

2.0 BACKGROUND AND OBJECTIVES

Cavitation erosion, in the past, has been a major problem for designers of hydrodynamic equipment. Realizing the enormous potential of this controlled phenomenon, a program was proposed to investigate the potential of cavitation as an underwater tool. By extrapolation of in-house data, calculations of anticipated cutting rates in steel utilizing controlled cavitation erosion were the basis for the proposed program.

Under the sponsorship of the Office of Naval Research, the initial program was undertaken to investigate the feasibility of controlled cavitation erosion cutting. A CONCAVER pumping system was assembled. The system was rated for 4.2 gpm flow at 7,500 psi maximum operating pressure. Figure 1 is the schematic diagram of the pumping system. The system was utilized to penetrate a 1/8" thick aluminum plate. Intensities of cavitation erosion were measured and the intensity-velocity-power law relationship was established. A direct relationship between intensity of erosion and cutting rate was established, and the specific measurement of intensity of erosion as a function of velocity was characterized. Measurements of velocity and intensity were used to predict cutting rates.

During the second phase of the program, the laboratory facility was expanded by the design of a second pump and additional laboratory equipment to measure associated nozzle parameters. The additional system was capable of 5 gpm flow at

12,000 psi operating pressure. This facility was used to extend the velocity power law relationship to 1,200 fps. A cutting rate in 1/4" thick aluminum plate was established of 1/2 inch per minute.

As a result of the successful accomplishments in the initial phases of the program, the current phase of the research program was established. The major objective of this phase of the program was to generate the necessary engineering data in order to maximize the intensity of erosion and the cutting rate potential of the CONCAVER system.

In order to reach this major objective, the program progressed in two major segments. The specific objectives were:

1. To evaluate the associated nozzle parameters of nozzle diameters, loss coefficient, nozzle velocity, nozzle pressure and nozzle offset distance in order to determine the effect on intensity of erosion and cutting rate.

2. To evaluate cutting rate in 1/2" thick aluminum plate based on the results of data accumulated:

3. To extend the operating pressure to 15,000 psi.

Additional objectives were established based upon analysis of the data generated. These objectives were:

1. To evaluate the effect of nozzle geometry on nozzle performance;

2. To optimize the single nozzle cutting rate for the CONCAVER facility;

3. To evaluate the cumulative effect on cutting rate utilizing dual nozzles;

4. To evaluate the effect on cutting rate at simulated water depths;

5. To establish cutting rates in 1/2" thick aluminum, based on nozzle optimization.

The test data in this report addresses the accomplishments of this phase.

3.0 EXPERIMENTAL APPARATUS AND TECHNIQUES

During the second phase of the program the laboratory facility was expanded in order to obtain increased velocities. In addition, laboratory equipment was required to measure the associated nozzle parameters. The equipment designed and assembled during the second phase was utilized for the experiments in Phase III. Figure 2 is the schematic diagram of the additional laboratory facility. The system is comprised of a triplex plunger pump, drive motor, control panel, test chamber and associated hardware. The pump is rated to operate to a pressure limit of 12,000 psi for a flow rate of 5 gpm. The pump is driven by a belt system from the electric motor which is rated at 60 horsepower. Modifications to this system have increased the operating capabilities of the pump to 15,000 psi pressure at a 5 gpm flow rate. These modifications were made in an effort to further expand the velocity capabilities.

The control panel was designed to incorporate the gauges, switches and valves required to operate the pump in conjunction with the test chamber. One portion of the panel contains all of the pump associated controls. The pump or nozzle pressure gauge, the supply suction pressure gauge, and the air supply pressure gauge were mounted on this portion of the panel. Also, the pump, air compressor and auxiliary power control switches were mounted in this portion. The second portion of the panel contained the equipment associated with the operation

of the test chamber. A flow meter, a chamber level indicator, three chamber pressure gauges and the required valving was mounted in this portion of the panel. Figure 3 is the control panel schematic diagram.

The test chamber was designed and assembled with two major capabilities: 1) the ability to rotate and position a specimen test plate with respect to a stationary nozzle; and 2) the ability to withstand increased pressures thereby simulating increased water depths. The chamber was designed to accept 6" x 6" test specimens and to accommodate nozzle distances up to 9". It was also designed for hydrostatic pressures of 1,500 psi. This capability would allow testing to simulated water depths of approximately 3,000 feet. View ports were an integral part of the test chamber. These ports allowed visual observations to be made while experiments were being conducted. Figure 4 is the design concept drawing of the test chamber and identifies the capabilities of the test chamber. Figure 5 is the schematic flow diagram for the complete CONCAVER test facility.

Additional laboratory apparatus consisted of the velocity calibration chamber which was designed for the sole purpose of improving the velocity measurement techniques. Figure 6 is the design drawing of the velocity chamber. Water enters the chamber through the nozzle and leaves the chamber through the discharge port. The discharge calculations determine the velocity and flow measurement.

An additional equipment modification was required for the dual nozzle testing. The access port of the test chamber was modified. This door incorporated the fittings which support the nozzle and the specimen rod. An additional fitting was installed in the door to allow a second nozzle to operate simultaneously. The fitting was installed such that the two nozzles cut on the same arc. As the specimen plate was rotated, the circle was cut by two nozzles 180 degrees apart. This modification is illustrated in Figure 7. The associated high pressure plumbing changes were also made so that both nozzles functioned simultaneously.

4.0 OPERATIONAL PROCEDURES

Each nozzle was tested and evaluated in terms of the four major nozzle performance parameters. These factors included:

1. Nozzle velocity, V_o, (in fps);
2. Loss coefficient, C_v, (nondimensional);
3. Breakthrough time, B_t, (seconds); and
4. Nozzle horsepower, HP_m, (horsepower).

The nozzle parameters were optimized with respect to nozzle distance (D_n), nozzle pressure (P_o), and nozzle diameter (D_o). The accumulated test data included the velocity calibration, and the intensity calibration.

The orifice diameter of each nozzle was accurately measured as an initial step. This information was important for technical documentation as well as velocity calibration. After the nozzle diameter had been recorded, the nozzle was installed in the velocity calibration chamber and the velocity calibration was determined. Additionally, the velocity and loss coefficient (C_v) information was obtained as the intensity calibration was performed.

4.1 The Velocity Calibration

Specific tests were designed in order to generate both the velocity-pressure and loss coefficient pressure relationships. With the nozzle in the calibration chamber, the pressure was increased in 1,000 psi increments from 1,000 psi to

15,000 psi. For each pressure increment, three flow rate measurements were recorded. The repeat measurements ensured accuracy and reproducibility of the data generated. Applying this data to equation [1], the nozzle velocity as a function of nozzle pressure was determined.

$$V_o = Q/A \qquad [1]$$

where:

V_o = nozzle velocity (fps)
Q = flow rate (gpm)
A = nozzle orifice area (in^2)

The second relationship developed from the velocity calibration data was the loss coefficient as a function of pressure. The loss coefficient (C_v) is defined by:

$$C_v = \frac{V_o}{V_{th}} \qquad [2]$$

where:

C_v = loss coefficient (nondimensional)
V_o = actual nozzle velocity (fps)
V_{th} = theoretical nozzle velocity (fps)

The theoretical velocity is defined as the velocity potential and is dependent on operating pressure. The following equation mathematically defines V_{th}:

$$V_{th} = \sqrt{2 \cdot g \cdot \Delta P} \qquad [3]$$

where:

V_{th} = theoretical velocity (fps)

g = gravitational force (ft/sec^2)

ΔP = pressure drop across the nozzle orifice (psi)

The velocities calculated from equation [1] are applied to equation [2], in order to obtain the corresponding pressure to calculate V_{th} from equation [3]. The loss coefficient, C_v, as a function of nozzle pressure can be calculated. This non-dimensional velocity coefficient is used as a performance indicator for the nozzle. An efficient nozzle will have a high C_v factor and will be constant with respect to pressure.

4.2 The Intensity Calibrations

The intensity calibrations were obtained from experiments utilized to determine the remaining parameters of interest for each nozzle examined. For these experiments, the test chamber was utilized. Intensity calibrations were performed at a chamber pressure of zero psi (sea level water depth). The nozzle was secured within the test chamber along with a test sample specimen. The sample material utilized for all intensity calibrations was 1/4" thick 1100-F aluminum plate, 6" square. This material was chosen because the erosion characteristics and erosion strength were known quantities. With this equipment installed, the chamber was sealed, flooded and testing initiated.

The intensity calibration measured breakthrough time (B_t), which was used to calculate intensity of erosion. Breakthrough time was measured as a function of nozzle distance for nozzle pressures in the range of 10,000 to 15,000 psi. At a specific pressure, the nozzle distance (D_n) was varied from 1/4" to 3/4". At each distance setting, three breakthrough times were measured. The additional measurements were made to ensure accuracy and reproducibility. In addition, a check on nozzle performance was made. For each adjustment of the distance setting, a flow rate measurement was made. This information was compared with the velocity calibration and previous measurements in order to ensure consistent nozzle operation. As each breakthrough time measurement was made, the test sample was rotated to a clear position to start the next data point.

The breakthrough time data was applied to the following equation which defines intensity of erosion:

$$I_e = \frac{i S_e}{t} \qquad [4]$$

where:

I_e = intensity of erosion (watts per meter^2)

i = erosion depth (thickness of sample plate) (in)

t = exposure time (breakthrough time measured) (sec)

S_e = erosion strength of the material (psi)

Calculated values of I_e were normally plotted as a function of nozzle pressure and/or nozzle distance.

The nozzle power parameter was obtained for each nozzle evaluated. Nozzle power was plotted as a function of nozzle pressure. Data obtained from both calibration tests was utilized to determine nozzle power from the following equation:

$$HP_m = \frac{Q\ \Delta P}{1714} \qquad [5]$$

where:

HP_m = measured nozzle power (np)

Q = nozzle flow rate for a given ΔP (gpm)

ΔP = pressure drop across the orifice (psi)

The nozzle power parameter was utilized for optimization and system design because the power requirement of the prototype field system can be established.

The velocity calibration chamber was not utilized for the double nozzle calibration because it would not accommodate two nozzles. Therefore, the velocity (C_v) and flow rate measurements were made in the test chamber. Intensity calibration data with two nozzles was gathered following the previously described procedures.

The effect on breakthrough time for increased water depth was investigated after the optimum nozzle diameter had been determined. The optimum nozzle and specimen plate were mounted

in the test chamber, and in order to minimize the number of variables; the optimum nozzle distance was set constant for the test duration. Three operating nozzle pressures were selected from 10,000 to 15,000 psi. At each nozzle pressure, a range of chamber pressures was examined from 0 to 50 psi which simulated water depths (d) from 0 to 115 feet. For each chamber pressure setting, the breakthrough time was measured.

5.0 EXPERIMENTAL RESULTS AND DISCUSSION

5.1 Nozzle Evaluations

Nozzles ranging in orifice diameter from 0.020 to 0.040 inches were tested. This testing occurred prior to system modification. For this reason, the maximum nozzle pressure reached with the initial series of nozzles was 12,000 psi. Figure 8 is an example of data obtained for each nozzle tested. From this data, optimum breakthrough time and nozzle distance was obtained for the nozzle being evaluated. For the 0.033 nozzle shown in Figure 8, the optimum distance was 0.48 inches and the optimum breakthrough time was 18 seconds. Similar data was gathered for each nozzle tested.

Figure 9 is the graphic summary of breakthrough time as a function of nozzle distance for the initial series of nozzles tested. The optimum distance for the 0.030 inch diameter nozzle was found to be 0.5 inches. Figure 10 illustrates the optimum breakthrough time as a function of nozzle diameter. This figure indicates the optimum breakthrough time obtained for each nozzle tested. Figure 11 is the optimum breakthrough time as a function of nozzle pressure for the nozzles tested. For a given nozzle pressure, Figure 11 will allow determination of the optimum breakthrough time obtained at pressure for each nozzle evaluated. Figure 12 is a design chart relating optimum breakthrough time and measured nozzle power to nozzle diameter for various operating pressures. The power

produced and associated breakthrough time can be determined from Figure 12 for any nozzle diameter and operating pressure combination. As an example, for an 0.030 nozzle at 12,000 psi, the power produced by the nozzle was 14 horsepower. The power rating of 14 horsepower generated breakthrough times of approximately 20 seconds.

At this time in the program, the laboratory experiments and the equipment were modified to produce 4.2 gpm at 15,000 psi nozzle pressure. Test procedures were identical for the second series of nozzles with the exception that the pressure range was extended to include 15,000 psi. Figure 13 is an example of the data gathered for each nozzle in this series. This figure indicates breakthrough times obtained for the 0.030 inch diameter nozzle as a function of nozzle distance at 12,000 psi nozzle pressure. The optimum distance was about 1/2 inch. The optimum breakthrough time had been reduced from approximately 20 seconds to approximately 10 seconds. A similar improvement in breakthrough time was noted for each nozzle in the series.

The additional data at 15,000 psi showed as additional reduction in breakthrough time. The breakthrough time curve flattened and remained constant as a function of nozzle distance. Figure 14 illustrates the data gathered. Breakthrough time was reduced to approximately 5 seconds and was nearly constant for distances from just under 1/2 inch to just over

5/8 inch. The flattened curve was significant because it indicated the ability to cut thicker materials at the same rate the 1/4 inch thick material was being cut. The information obtained while testing this series of nozzles led to the attempts to cut 1/2 inch thick aluminum rate. Figure 15 illustrates the data. For the optimum nozzle distance, which was approximately 1/2 inch, the optimum breakthrough times were plotted as a function of nozzle diameter for both 12,000 and 15,000 psi. The data indicated the minimum breakthrough time occurred for a nozzle diameter of 0.030 inches. The optimum breakthrough time obtained for that nozzle was 10 seconds at 12,000 psi and 5 seconds for 15,000 psi.

The summary chart (design chart) shows optimum breakthrough time and nozzle power as a function of nozzle diameter. Figure 16 is that chart for this series of nozzles. Figure 16 indicates that the optimum breakthrough time occurred for a nozzle power of approximately 22 horsepower. The optimum breakthrough time was obtained with only 1/2 of the total power available with the system. This testing allowed the cutting rate in 1/2 inch thick aluminum plate to be established at 5/8 inch per minute as indicated in Figure 17.

The testing proceeded and basic data was gathered for a third series of nozzles ranging in diameter from 0.020 to 0.040 inches. Figure 18 is the velocity curve for the 0.033 inch diameter nozzle as a function of pressure for pressures

ranging from 10,000 to 15,000 psi. This data showed the steady progressive increase of velocity with respect to pressure. Figure 19 is the corresponding loss coefficient (C_v) data. The C_v data indicated a slightly lower performance for this series. However, the loss coefficient remained constant over the pressure range. The data was obtained for nozzle pressures from 10,000 to 15,000 psi.

Breakthrough time data was also gathered for the nozzle series. Figure 20 illustrates the breakthrough time data for the 0.033 inch diameter nozzle at 15,000 psi. Similar data was gathered until the complete diameter range had been calibrated. The first summary curve generated the comparative loss coefficient factors of the nozzles tested. Figure 21 illustrates the performance factors of the nozzles tested. Additional summary curves relating optimum breakthrough time to initial nozzle pressure and nozzle diameter are given in Figures 22 and 23. From Figure 22, the optimum diameter was seen to be 0.033 inches. This nozzle delivered breakthrough times of 10 seconds or less. Figure 25, which relates breakthrough time to diameter directly, graphically illustrates the performance of each nozzle for three pressures. Figure 24 shows the optimum breakthrough time and measured nozzle power as a function of nozzle diameter for this series of nozzles.

The 0.040 inch diameter nozzle was important because this nozzle utilized all of the available power of the system.

Figures 25 and 26 are the respective velocity calibration and loss coefficient curves for the 0.040 inch diameter nozzle. From the velocity calibration, the velocity of the 0.040 nozzle at 15,000 psi was approximately 1100 fps. The flow rate for this nozzle indicated 90% of the available flow was passing through the orifice. Utilizing equation [5], the horsepower measured at the nozzle was found to be approximately 41 horsepower.

Figure 27 graphically illustrates the breakthrough time as a function of nozzle distance for the 0.040 inch diameter nozzle at 15,000 psi. The breakthrough time did not maintain distance independence. The breakthrough time increased beyond 5/8 inch nozzle distance. The minimum breakthrough time obtained was approximately 15 seconds. The optimum breakthrough time as a function of nozzle diameter was obtained with the 0.033 inch diameter nozzle. The complete design chart expressing the total capabilities of the CONCAVER system with a single nozzle was assembled. Figure 28 illustrates the optimum nozzle for the CONCAVER system. Utilizing the information in the design chart, and the limitations of the flow system, an evaluation of dual nozzle testing was initiated.

5.2 Dual Nozzle Testing

The CONCAVER system was capable of a 5 gpm flow rate at 15,000 psi. By calculation, two 0.033 inch nozzles would not reach 15,000 psi because one nozzle of that diameter would

require more than 50% of the total flow potential. Therefore, the 0.025 inch diameter was chosen because two nozzles would accommodate the flow and reach maximum pressure. The modifications previously described were incorporated into the system for dual nozzle testing. After modification of the facility, testing followed the same procedures as before. Each nozzle was calibrated independently to ensure individual characteristic response. A velocity calibration was performed. The double nozzle system was installed in the test chamber and the velocity calibration was repeated.

The velocity calibration data showed that the two nozzles were actually passing more flow than had been calculated, but not in excess of the system limit. Figure 29 is the velocity calibration curve for the two nozzle system. The maximum velocity attained was approximately 1150 fps. This velocity was slightly higher than predicted, but predictions were based on an assumed C_v factor. Figure 30 illustrates the actual loss coefficient data obtained as a function of nozzle pressure. The two nozzles operated with a loss coefficient of 0.77, which was comparable to the single nozzle value. Additional information gathered from the velocity calibration indicated that the two nozzles produced approximately 30 horsepower at 15,000 psi nozzle pressure.

The intensity calibration of the dual nozzle system generated breakthrough times which were in the range predicted.

An optimum distance of approximately 5/8 inch was obtained. However, the dual nozzle system breakthrough time was not constant with respect to distance. Breakthrough time increased abruptly beyond 5/8 inch nozzle distance. Figure 31 illustrates the breakthrough time was approximately 13 seconds. The breakthrough time increased as a result of using less than an optimum nozzle diameter, but twice the material was removed. The increase in breakthrough time did not reduce the associated cutting rate. Cutting rate data was gathered with the dual nozzle system on a 1/2 inch thick aluminum plate. A new cutting rate for 1/2 inch aluminum was established. That rate was 1-1/16 inches per minute. Figure 32 graphically summarizes the cutting rate information obtained.

5.3 Evaluation of the Effect of Water Depth

The optimum single nozzle diameter of 0.033 was utilized in examining the effect of increased depth on nozzle performance. Since the cavitating envelope of the jet is a function of chamber pressure, a constant nozzle distance was used. However, this provided less than optimum conditions as higher chamber pressures were tested. Nevertheless, the effect on breakthrough time was solely dependent upon water depth.

A chamber pressure range from 0 to 50 psi was selected. This pressure range simulated water depths from 0 to 115 ft. Nozzle pressures of 10,000, 12,000 and 15,000 psi were evaluated. Figure 33 is the graphic representation of the water

depth data gathered. Examination of Figure 33 indicated that at 15,000 psi and 90 feet of water depth, a 46% improvement in breakthrough time was realized.

5.4 Aluminum to Steel Conversion Factor

The development of an aluminum to steel breakthrough time conversion factor was the final data gathering activity of Phase III. The sample specimens to be tested were subjected to Rockwell hardness tests in order to specifically identify the specimens utilized. The aluminum specimen was Rockwell number 15T-15 and the steel specimen was Rockwell number 30T-56.

In separate tests, each specimen was mounted in the chamber and breakthrough times were measured. Constant nozzle parameters of distance, diameter and pressure were utilized. A nozzle of optimum diameter was used (0.033 inch). A nozzle distance of 1/2 inch was maintained. The tests were conducted at 15,000 psi nozzle pressure. Five breakthrough time measurements were made in each sample for the above conditions. The average of the five breakthrough time measurements were calculated and used as is illustrated in Figure 34. By dividing the breakthrough time for steel by the breakthrough time for aluminum, the conversion factor was established. This factor indicates the degree of improvement required to cut steel at the present cutting rate of aluminum. The projected achievement of this factor was based on increased velocity potentials and the improvements resulting from water depth. The increased

intensity of erosion should be higher than required by the indicated factor. Figure 35 illustrates the projected velocity-power law relationship. This figure illustrates the velocities required to increase intensity of erosion by a factor of 80. The increased intensities indicated from Figure 35 are related to velocity only. Additional increases in intensity should occur as a result of water depth. However, the effect of water depth on the intensity of erosion has not yet been fully developed.

6.0 SUMMARY OF TECHNICAL ACCOMPLISHMENTS

The technical accomplishments of the program have been dependent on previous accomplishments. As a result, the accomplishments discussed in this section are listed in Figure 36. First, the single nozzle testing was extended to the limit of the CONCAVER system. The optimum single nozzle was determined to be in the orifice range from 0.030 to 0.033 inches, depending on the associated loss coefficient. The optimum nozzle distance was found to be from 1/2 to 5/8 inch. At the above setting, the optimum nozzle developed breakthrough times from 5 to 10 seconds, at a nozzle pressure of 15,000 psi. The associated intensity of erosion that the nozzle developed was approximately 21,000 watts per meter squared. The power measured for this nozzle was 22 horsepower.

The second major accomplishment dealt with dual nozzle testing. A less than optimum nozzle diameter was selected and cutting rates determined for dual nozzle cutting. Breakthrough time measurements were gathered for the dual nozzle system. Based on breakthrough time information, the two nozzles were utilized to determine a new cutting rate in 1/2 inch thick 1100-0 aluminum plate. The new cutting rate was established at 1-1/16 inches per minute.

The third accomplishment was the initiation of investigation into the effects of cutting at different water depths. Although the initial experiments were not designed to optimize

the performance at water depths, the testing indicated an improvement in nozzle performance. The initial improvement observed at 15,000 psi nozzle pressure was approximately 46%.

The final accomplishment was the development of the aluminum to steel breakthrough time conversion factor. The conversion factor was determined in order to define the exact requirements remaining in the development of the CONCAVER technique. In order to cut steel at a rate comparable to the rate developed for aluminum, the current capabilities must be increased by a factor of 80. A method for obtaining this increase was also developed and appears in Figure 35. The projected region of the velocity power law relationship indicated the increase in velocity required to obtain a factor of 80 increase in intensities developed by the system. Knowledge of the requirements remaining have led to certain recommendations with respect to further technical development of the CONCAVER technology in order to cut steel underwater.

7.0 COMPARATIVE EVALUATION OF CUTTING TECHNIQUES

In order to establish a relative scale for the comparative evaluation of different cutting techniques, the current CONCAVER technology was compared with other state-of-technology cutting methods in operation (6,7). The basic characteristics of the three most widely employed underwater cutting techniques have been assembled and compared with the CONCAVER. The comparative information is illustrated in Figure 37. This figure illustrates the operating advantages and disadvantages generally described for each technique (8).

A thorough study of Figure 37 indicates two very distinct advantages to the CONCAVER technique. The first is the elimination of the hazard due to electric shock. The systems which now generate the optimum cutting rates can be very hazardous, if not fatal, if great care and safety are not exercised. The second advantage is the elimination of the danger of exploding trapped materials such as gasoline, fuel oil, ammunition, etc. All of the other techniques utilize some form of heating system which is potentially capable of exploding the aforementioned materials. The CONCAVER system does not use a dangerous heating method and therefore poses no danger of exploding trapped materials.

The CONCAVER system is at the threshold of moving from laboratory system to field operational hardware. Additional

advantages may develop as the transition takes place. However, the characteristics outlined in Figure 37 show a system which already exhibits some very beneficial traits.

8.0 CONCLUSIONS AND RECOMMENDATIONS

8.1 Conclusions

As the data has been gathered, many questions have been answered. With each additional experiment, the knowledge of the CONCAVER system has been advanced, developed, expanded and refined. The experimental results of Phase III have led to the following conclusions:

1. An orifice diameter of 0.030 inch, for a 1/2 inch nozzle distance and 15,000 psi nozzle pressure, developed a breakthrough time of 5 seconds in 1/4 inch aluminum plate;

2. The velocity obtained for the optimum nozzle was approximately 1200 fps at 15,000 psi.

3. For optimum nozzle diameters ranging from 0.030 inch to 0.033 inch, the loss coefficient was in the range of 0.65 to 0.90;

4. The optimum nozzle at 15,000 psi nozzle pressure produced a breakthrough time of approximately 10 seconds which was independent of nozzle distance from approximately 7/16 inch, to approximately 11/16 inch;

5. For the optimum nozzle intensity of cavitation erosion increased from 1.0×10^3 watts per meter

squared at 10,000 psi to 2.1×10^4 watts per meter squared at 15,000 psi;

6. The optimum nozzle produced 5 second breakthrough times while only utilizing 1/2 of the horsepower available;

7. The cutting rate obtained by trading optimum diameter for dual nozzle operation is 1-1/16 inches per minute in 1/2 inch thick aluminum plate;

8. At 15,000 psi nozzle pressure, increasing water depth to 90 feet creates a 46% increase in breakthrough time.

9. The intensities of cavitation erosion for nozzles examined to date vary as the twelfth power of velocity for the velocity range from 750 fps to 12,000 fps.

8.2 Recommendations

The data analysis, in addition to allowing certain conclusions to be stated, has provided certain recommendations. Areas of improvement have been indicated and based on the data gathered and analyzed, the following recommendations can be made:

1. It is recommended that complete modification be performed on the 30-5 CONCAVER unit to allow it to operate at maximum capability. This unit will serve as supply system for both laboratory and field operation;

2. It is recommended that an intensive investigation of cutting at water depths be performed. Optimum nozzle cutting rates, nozzle distances, and nozzle pressure with respect to water depths from 0 to 500 feet must be obtained;

3. It is recommended that the velocity-power law relationship be established for nozzle velocities from 1100 fps to 2500 fps;

4. It is recommended that a concentrated study be made to establish methods of increasing nozzle loss coefficients;

5. It is recommended that current nozzle designs be accepted as the standard designs;

6. It is recommended that continued optimization and system capability advances be based upon test results with a single nozzle configuration;

7. It is recommended that design, development and fabrication efforts be directed toward the required field demonstration hardware and equipment. These designs must be guided by factors of durability, ease of operation, optimum performance and safety;

8. It is recommended that the design data acquired and hardware fabricated during the proposed program be utilized to perform a field demonstration cutting steel underwater.

REFERENCES

1. A. P. Thiruvengadam, "Cavitation Erosion," Applied Mechanics Reviews, March 1971.

2. A. P. Thiruvengadam, "Prevention and Cure of Cavitation Erosion," Naval Research Reviews, May 1972.

3. Rouse, H., Howe, J. W., and Metzler, D. E., "Experimental Investigations of Fire Monitors and Nozzles," Trans. ASCE, Vol. 117, 1952.

4. A. P. Thiruvengadam, "Cavitation Inception and Damage," M. Se. Thesis, Department of Power Engineering, Indian Institute of Science, Bangalore, India, 1959.

5. A. P. Thiruvengadam, "Scaling Laws for Cavitation Erosion," Proe. Syns, on Flow of Water at High Speeds, International Union of Theoretical and Applied Mechanics, Lenigrad, 1971

6. Supervisor of Diving, U. S. Navy, "Technical Manual - Underwater Cutting and Welding," Navships Publication 0929-000-8010, Washington, D. C., November 1969.

7. Masubuchi, K., "Materials for Ocean Engineering," The M. I. T. Press, Cambridge, Massachusetts, June 1972.

8. Myers, J. J., "Handbook of Ocean and Underwater Engineering," - McGraw - Hill Book Company, New York, 1969.

DAEDALEAN ASSOCIATES, Inc.

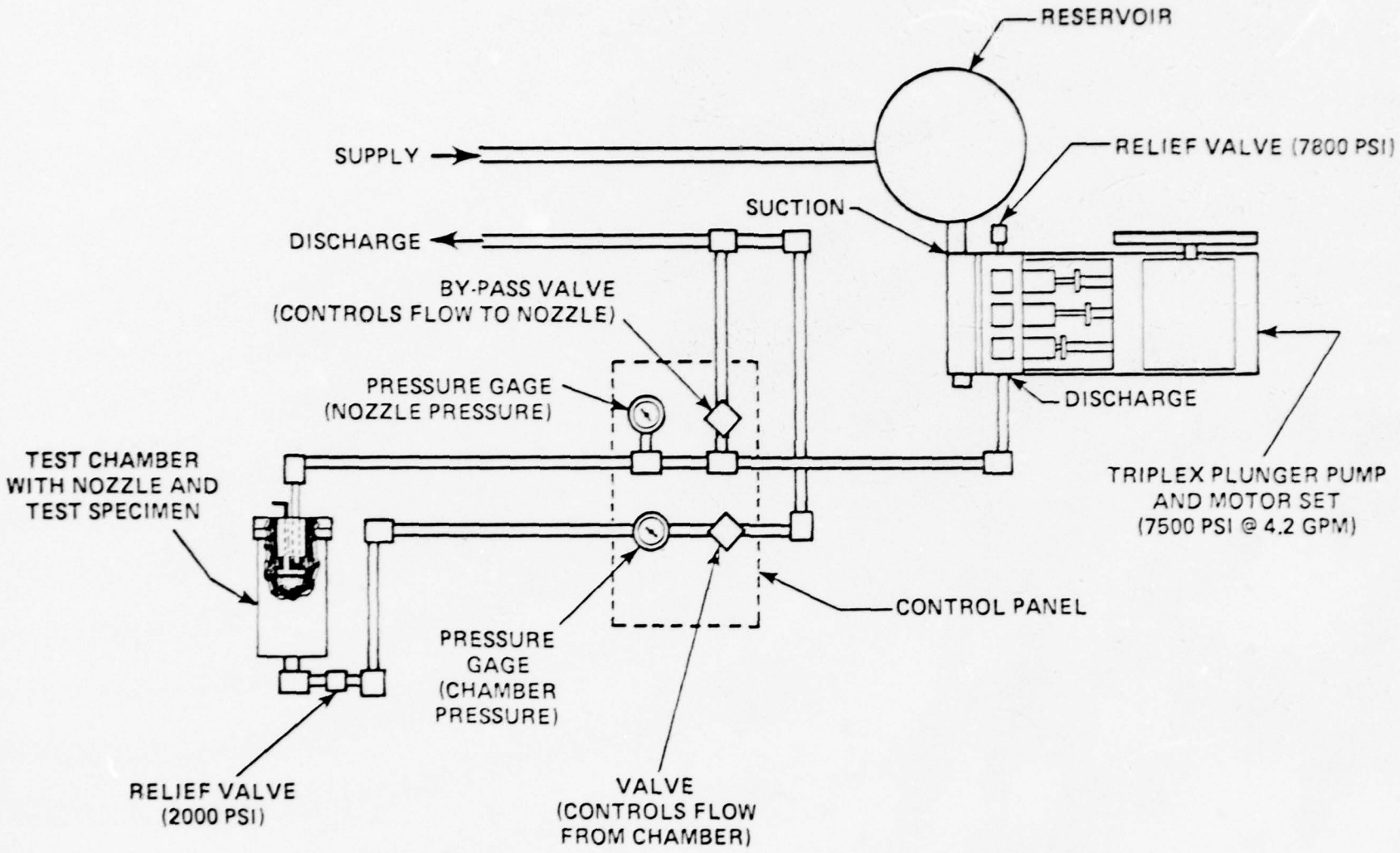

FIGURE 1 SCHEMATIC DIAGRAM OF DAI CONCAVER TEST FACILITY SHOWING THE SUPPLY AND DISCHARGE FLOW DIAGRAM AND BY-PASS CONTROLS

DAEDALEAN ASSOCIATES, Inc.

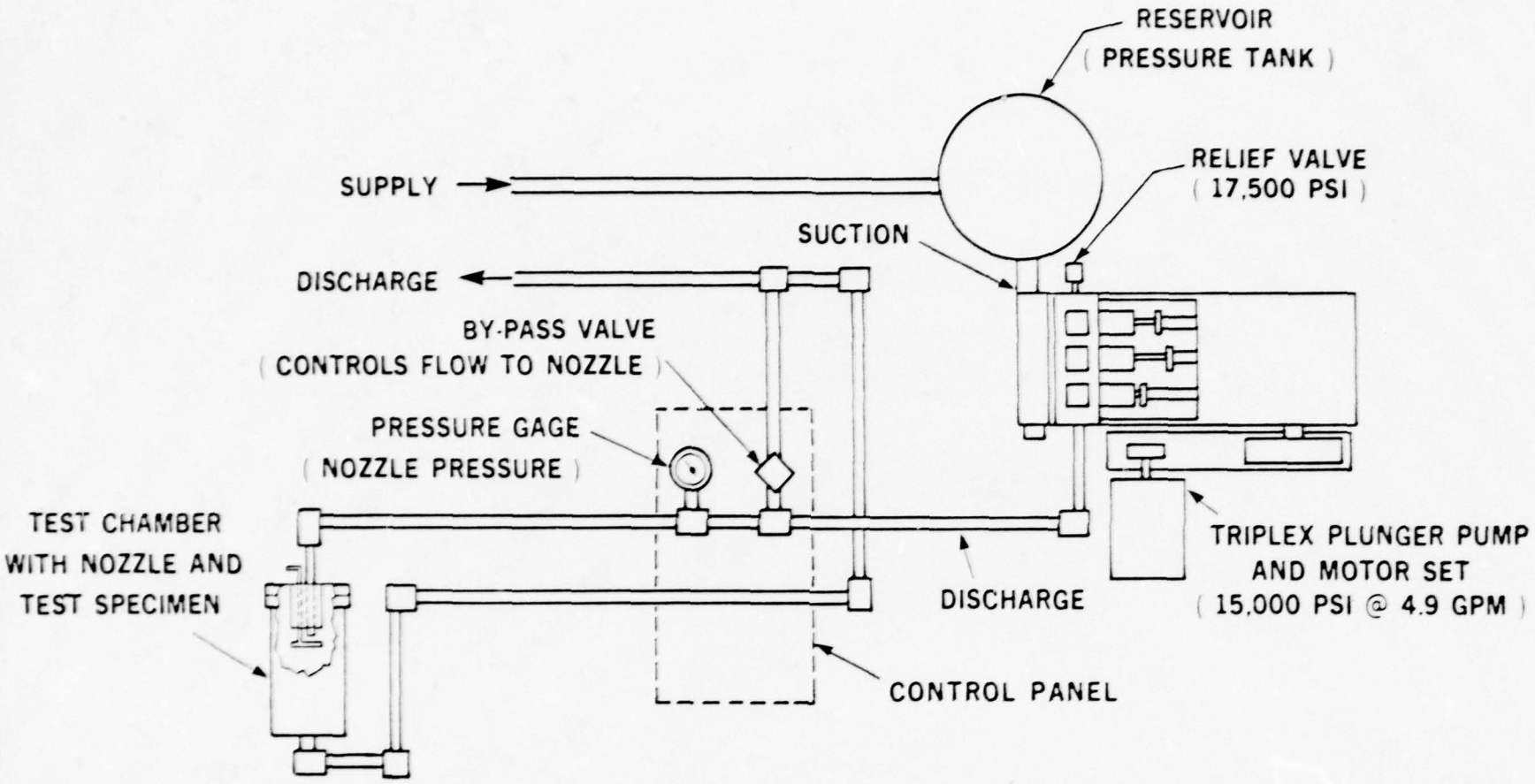

FIGURE 2 SCHEMATIC DIAGRAM OF DAI CONCAVER LABORATORY TEST FACILITY (**AS ASSEMBLED PHASE II**) SHOWING THE SUPPLY AND DISCHARGE FLOW DIAGRAM AND BY-PASS CONTROLS

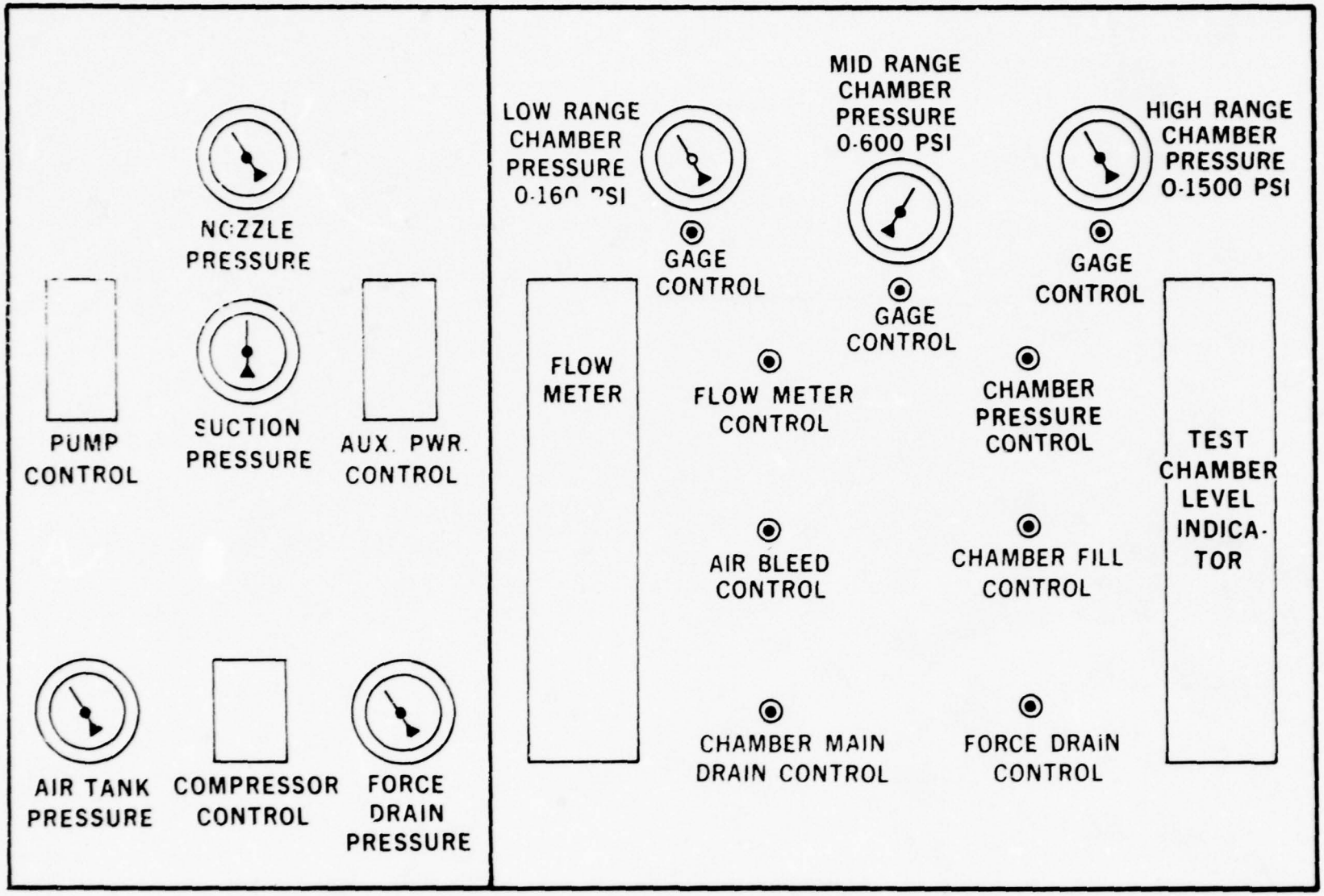

FIGURE 3 SCHEMATIC OF CONTROL PANEL FOR CONCAVER II TEST FACILITY

DAEDALEAN ASSOCIATES, Inc.

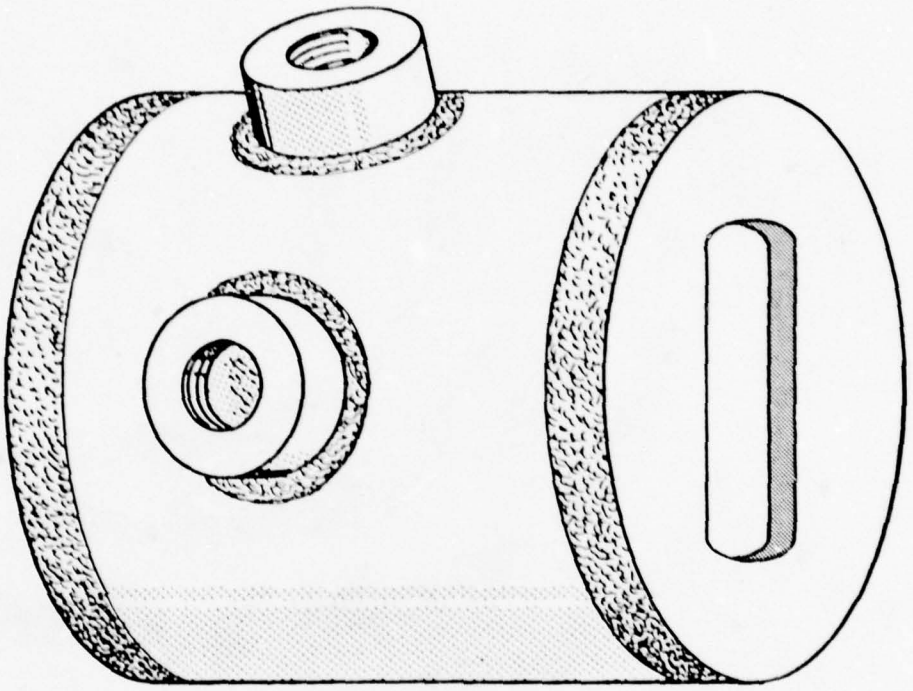

- SPECIMEN SIZE UP TO 6"×6"
- PRESSURE CAPABILITY UP TO **1500** psi
- SPECIMEN DISTANCE UP TO 9"
- VIEW PORTS FOR BASIC RESEARCH

FIGURE 4 DESIGN CONCEPT DRAWING OF THE CONCAVER II SYSTEM TEST CHAMBER WITH VIEW PORTS AND ITS CAPABILITIES

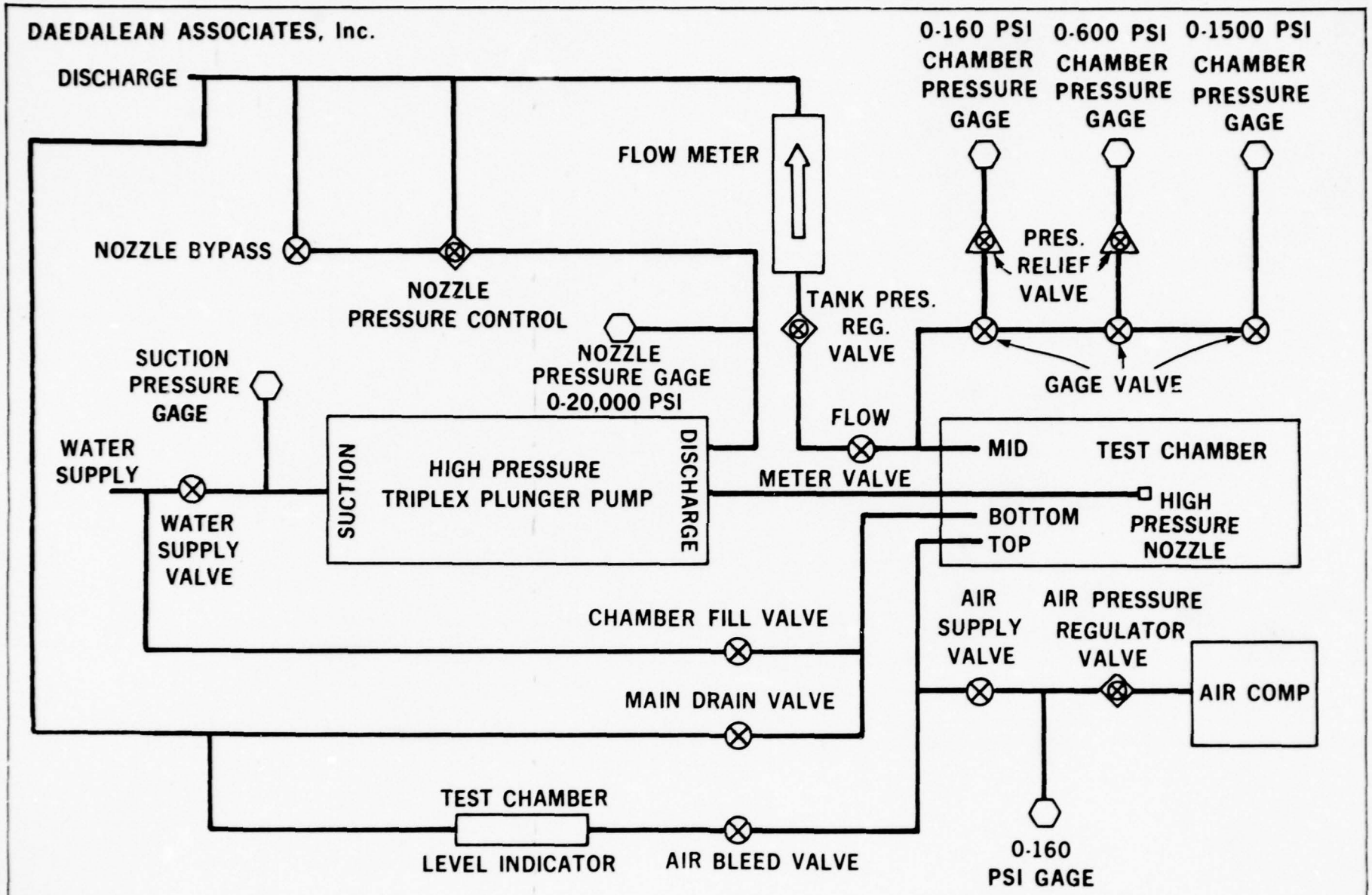

FIGURE 5 A SCHEMATIC FLOW DIAGRAM FOR THE CONCAVER II TEST FACILITY

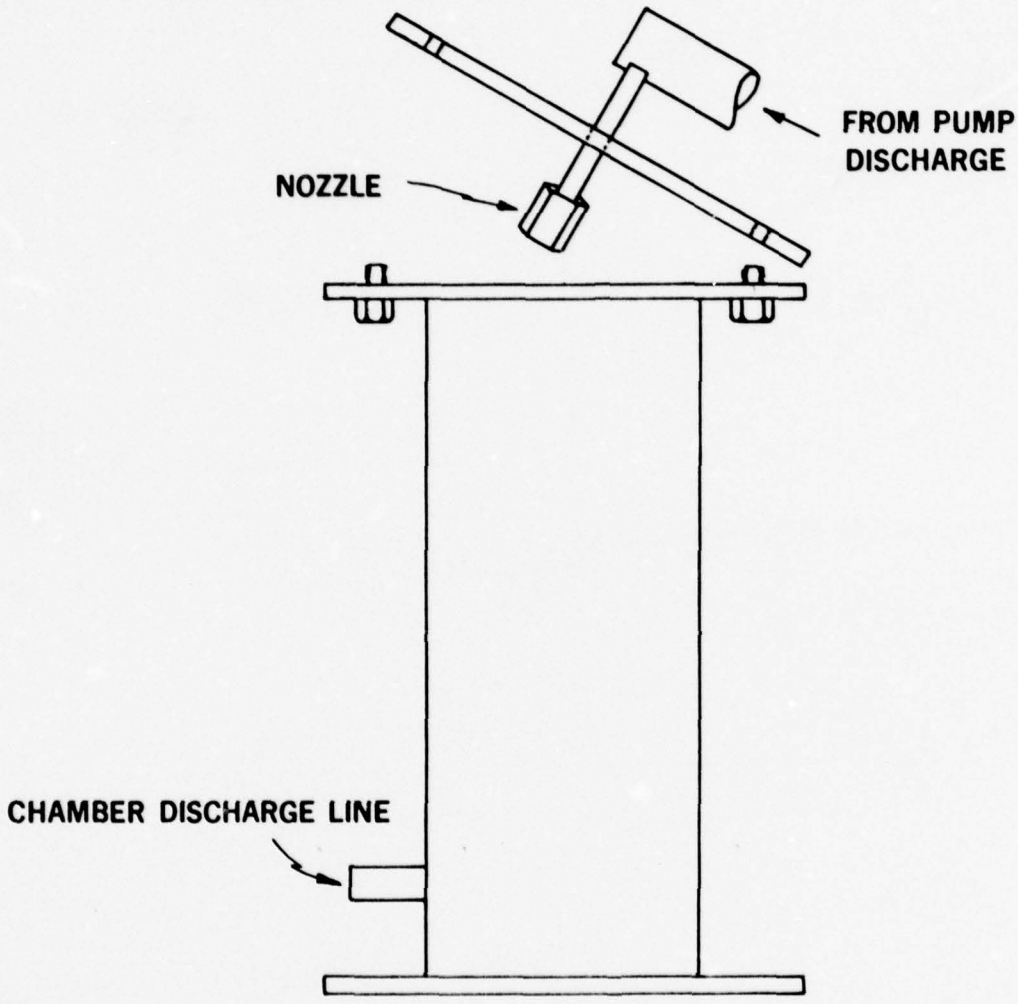

FIGURE 6 DESIGN CONCEPT DRAWING OF THE VELOCITY CALIBRATION CHAMBER

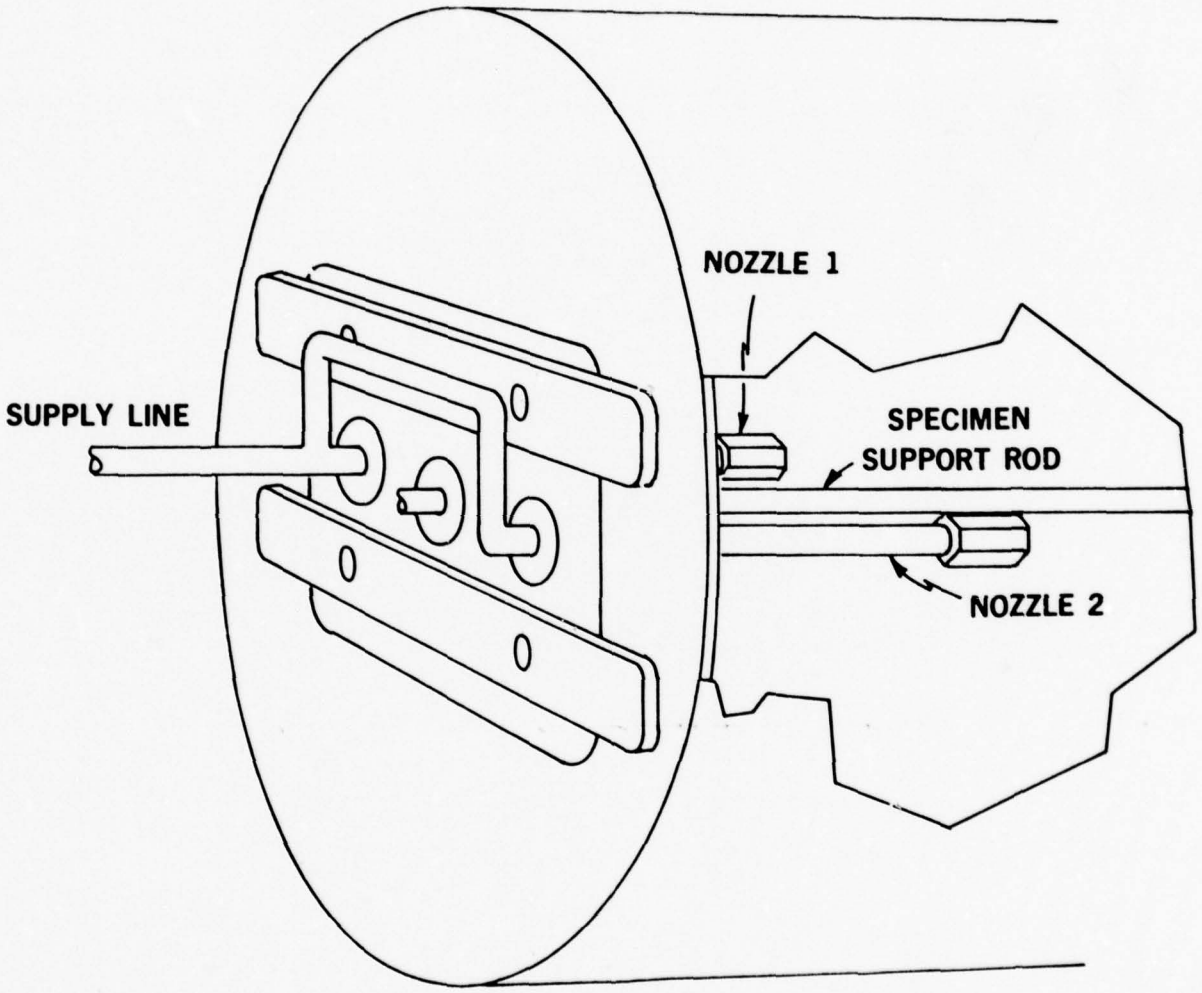

FIGURE 7 ILLUSTRATION OF DUAL NOZZLE CUTTING SYSTEM AS ASSEMBLED ON TEST CHAMBER REAR DOOR

DAEDALEAN ASSOCIATES, Inc.

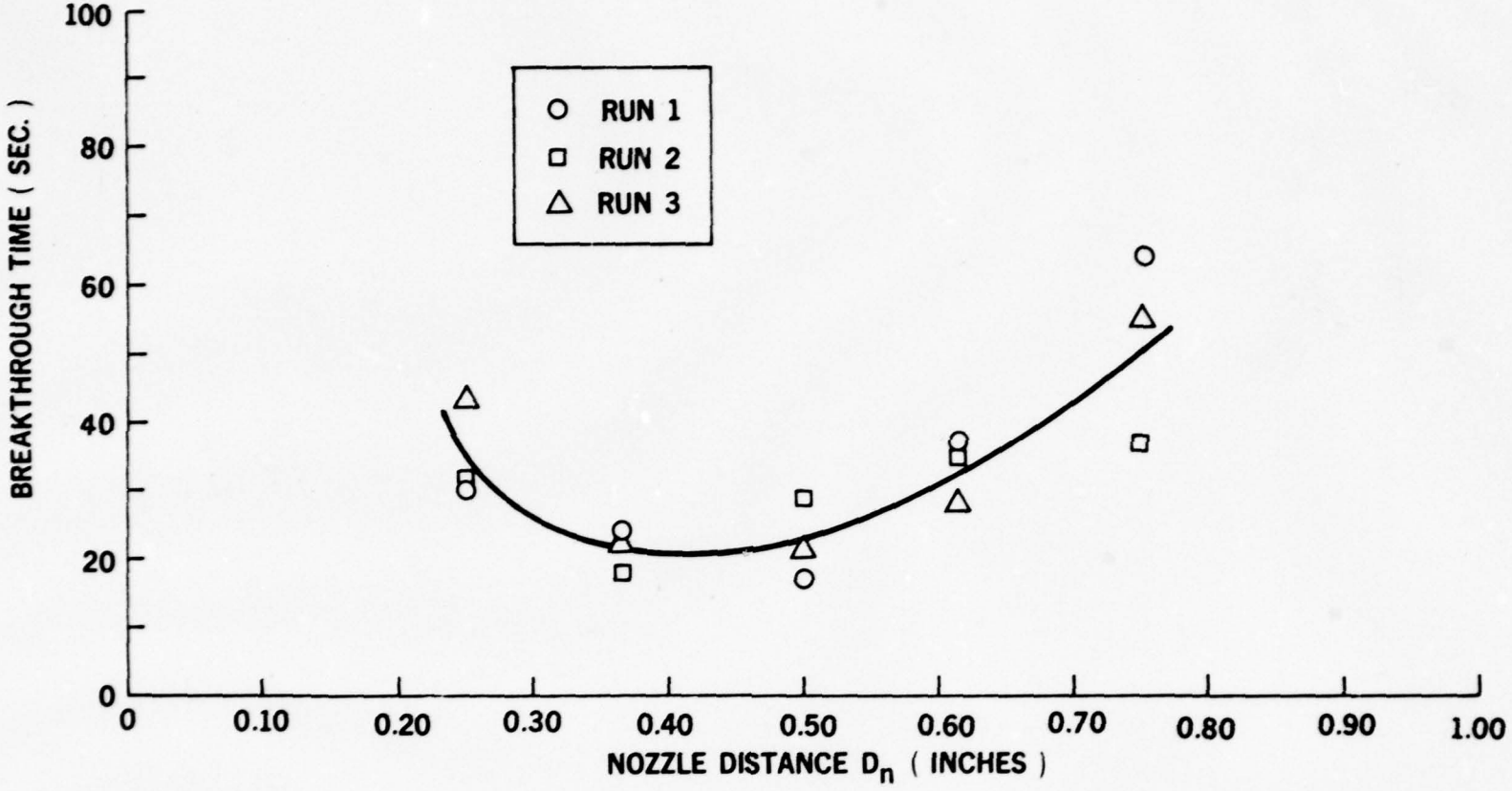

FIGURE 8 BREAKTHROUGH TIME AS A FUNCTION OF NOZZLE DISTANCE DISTANCE FOR 0.033 INCH DIAMETERS NOZZLE AT 12,000 PSI NOZZLE PRESSURE

DAEDALEAN ASSOCIATES, Inc.

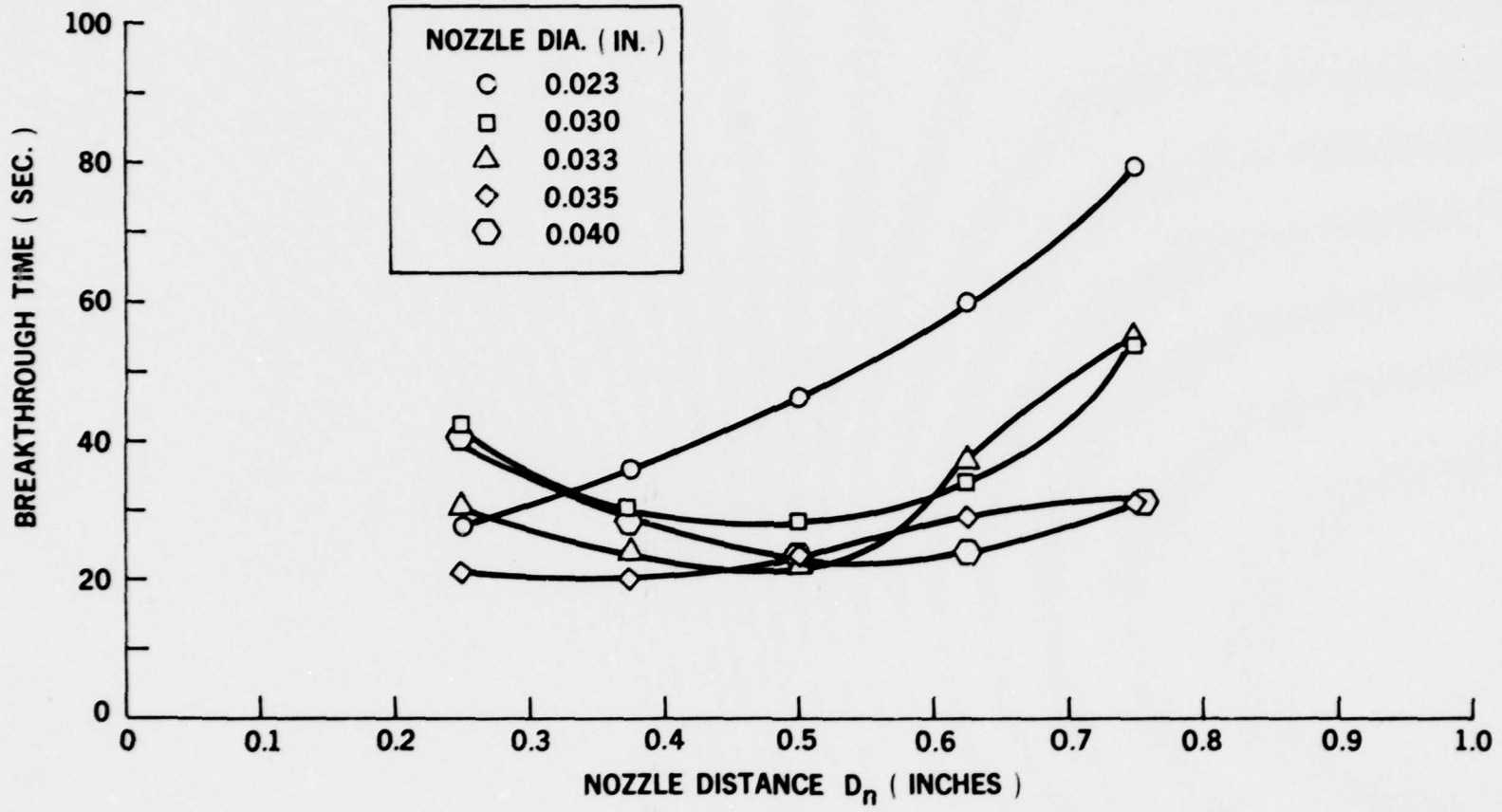

FIGURE 9 SUMMARY OF BREAKTHROUGH TIME AS A FUNCTION OF NOZZLE DISTANCE FOR VARIOUS NOZZLE DIAMETERS AT 12,000 PSI NOZZLE PRESSURE

DAEDALEAN ASSOCIATES. Inc.

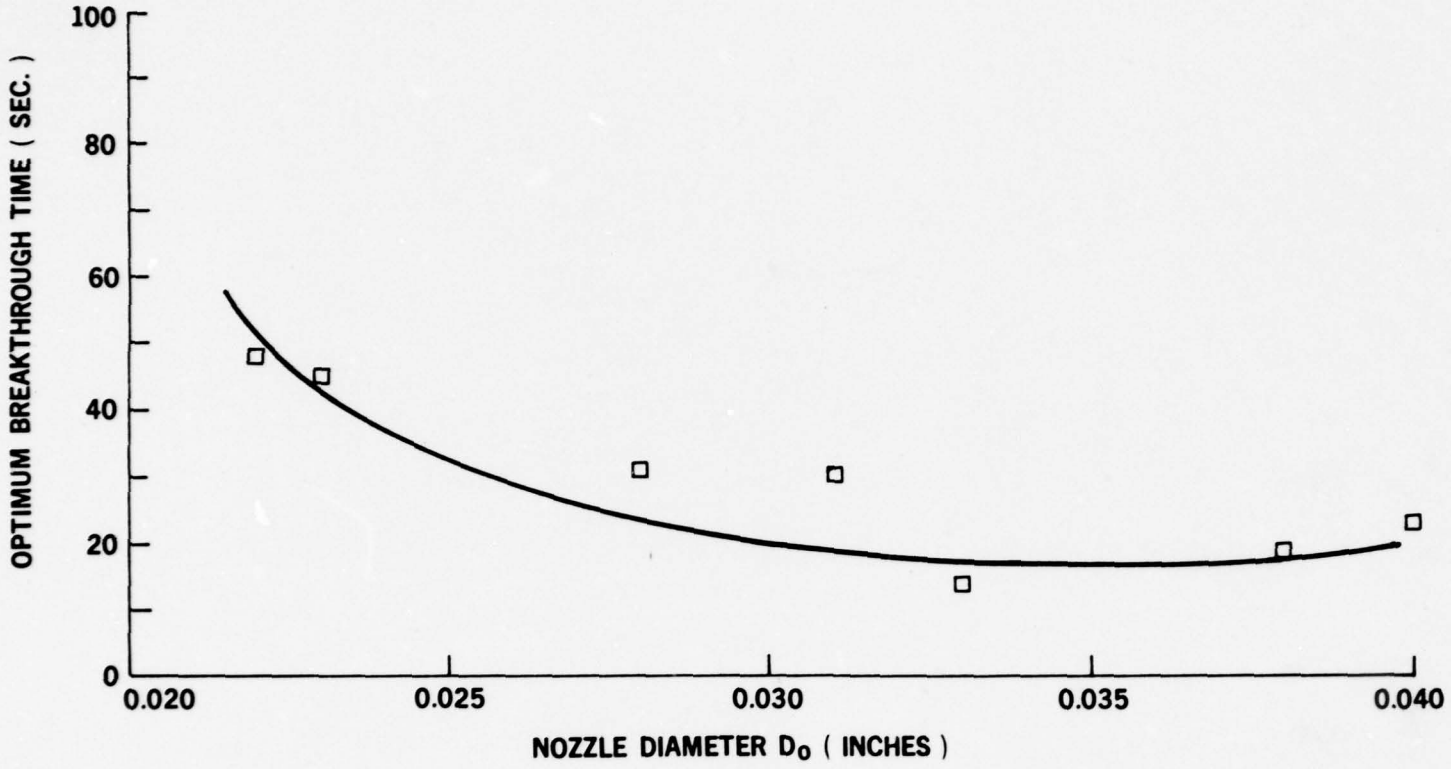

FIGURE 10 OPTIMUM BREAKTHROUGH TIME AS A FUNCTION OF NOZZLE DIAMETER AT OPTIMUM NOZZLE DISTANCE & AT 12,000 PSI NOZZLE PRESSURE

DAEDALEAN ASSOCIATES, Inc.

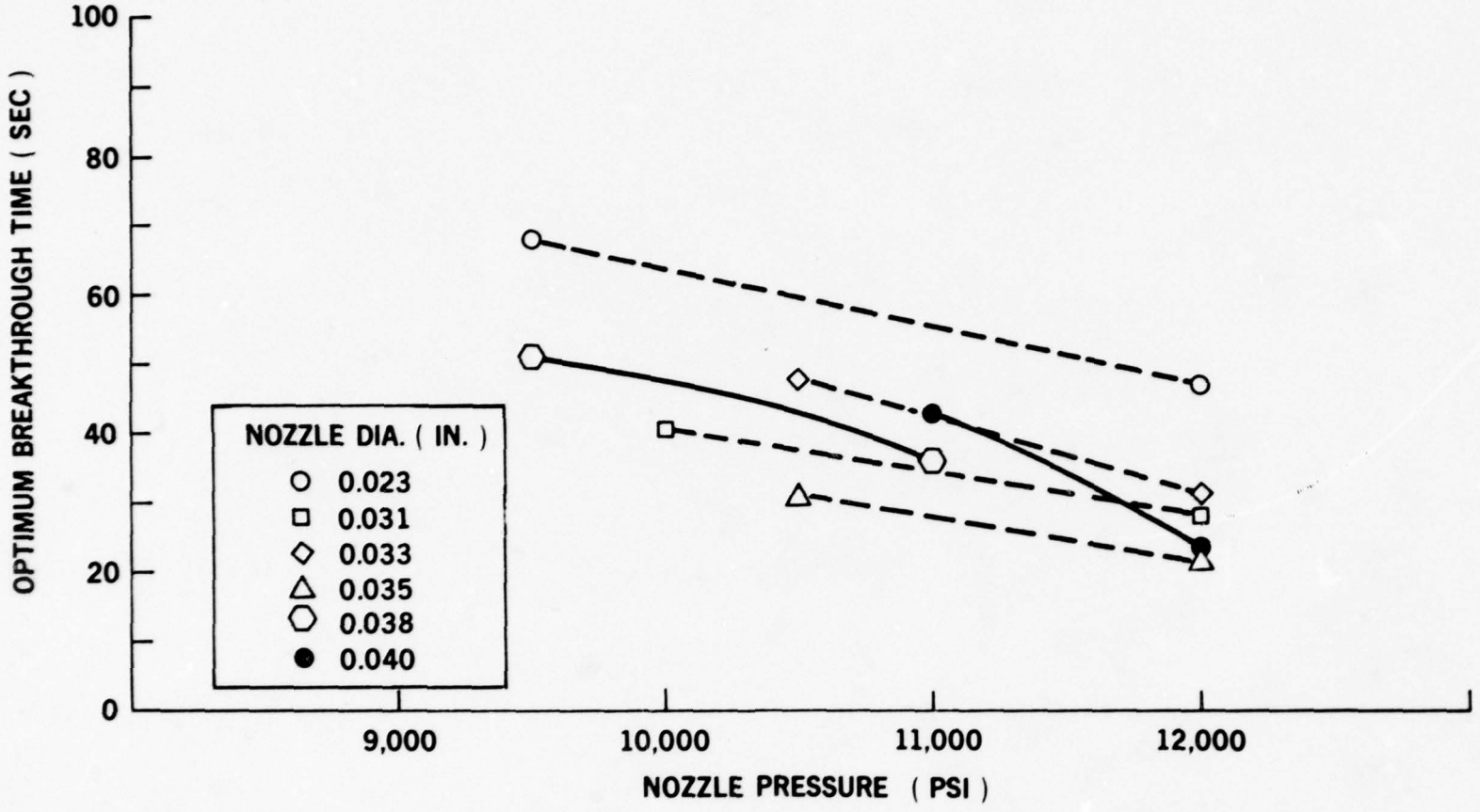

FIGURE 11 SUMMARY OF OPTIMUM BREAKTHROUGH TIME AS A FUNCTION OF NOZZLE PRESSURE FOR VARIOUS NOZZLE DIAMETERS

DAEDALEAN ASSOCIATES, Inc.

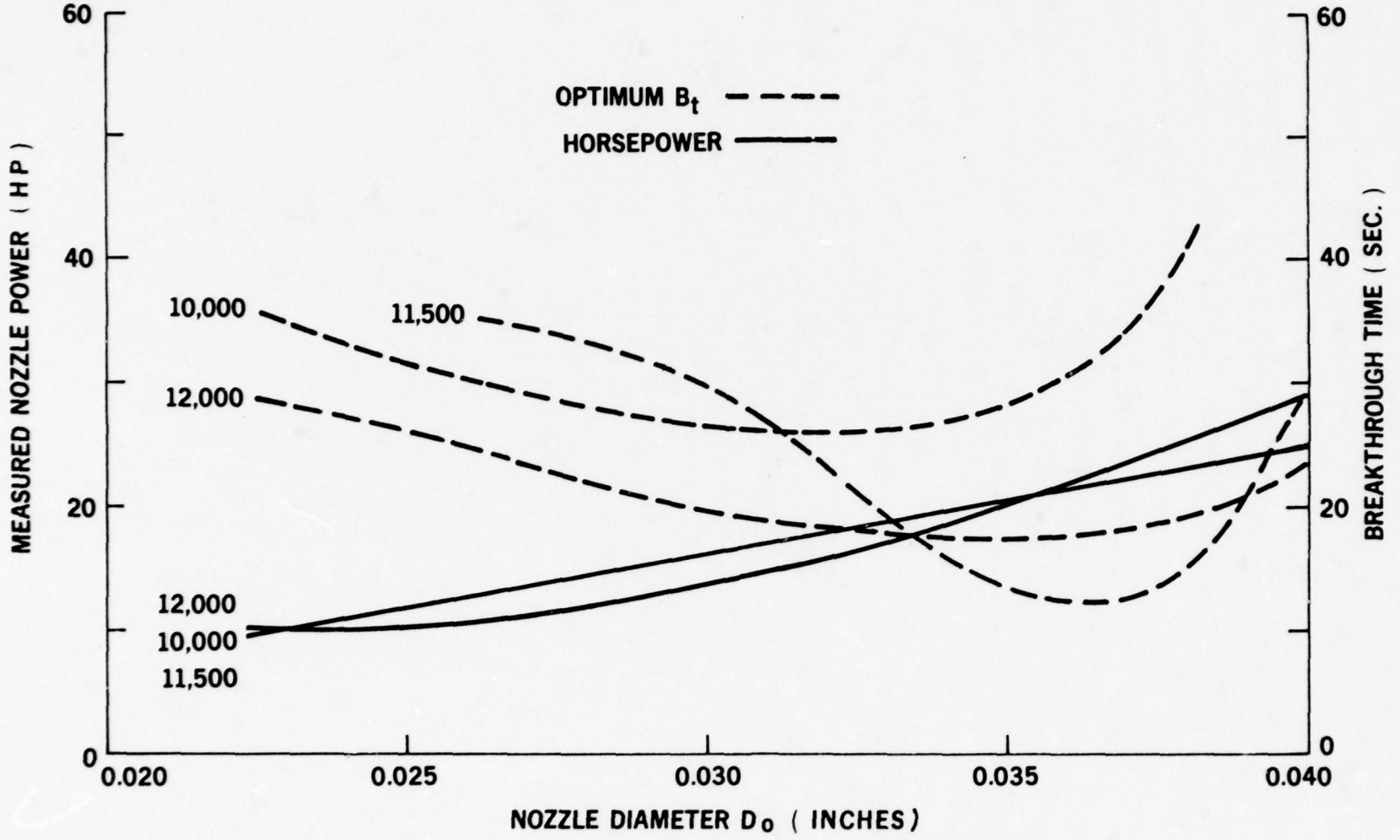

FIGURE 12 OPTIMUM BREAKTHROUGH TIME AND MEASURED NOZZLE POWER AS A FUNCTION OF NOZZLE DIAMETER FOR THREE OPERATING PRESSURES

DAEDALEAN ASSOCIATES, Inc.

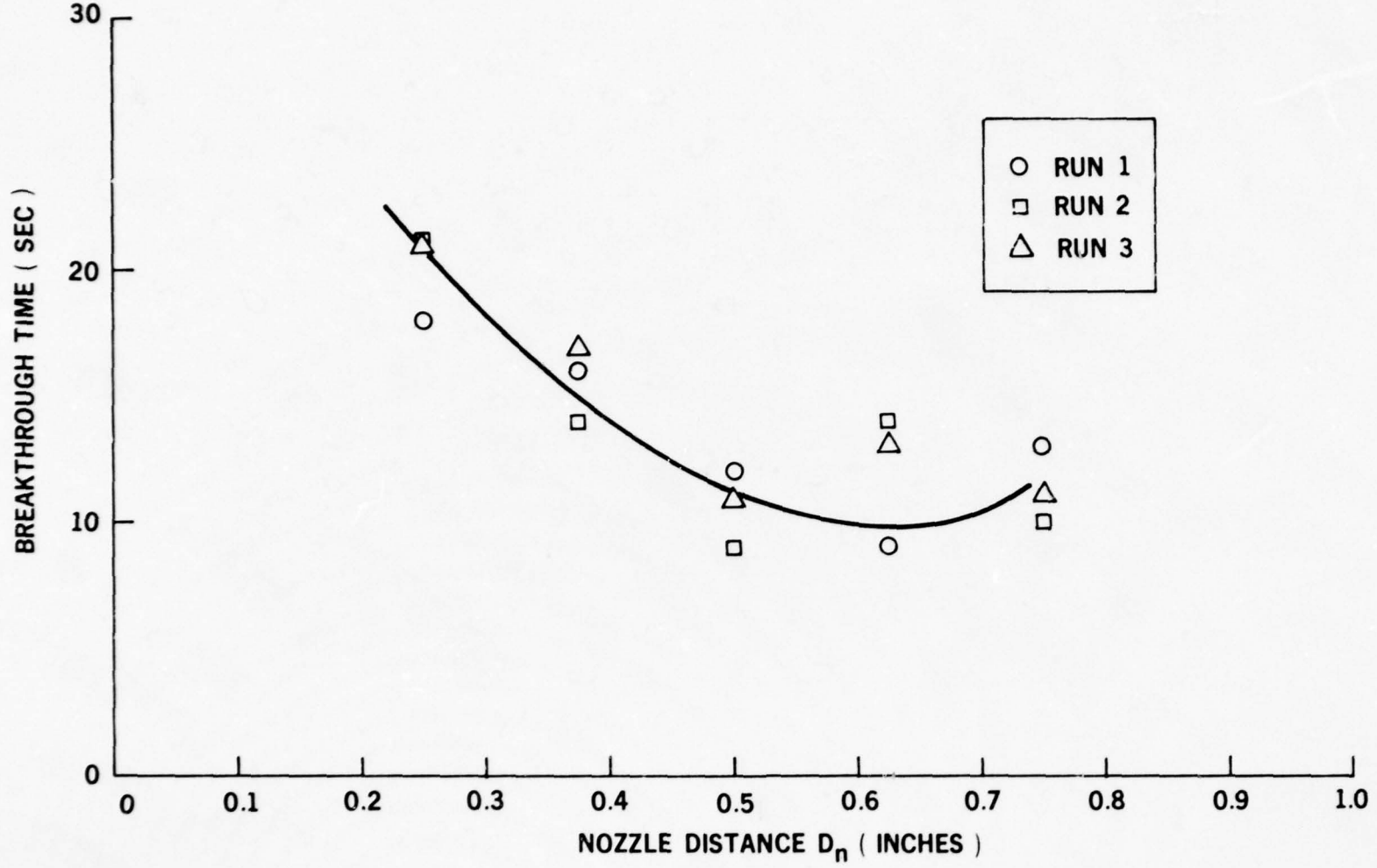

FIGURE 13 BREAKTHROUGH TIME FOR 0.030 INCH NOZZLE AS A FUNCTION OF NOZZLE DISTANCE AT 12,000 PSI NOZZLE PRESSURE

DAEDALEAN ASSOCIATES, Inc.

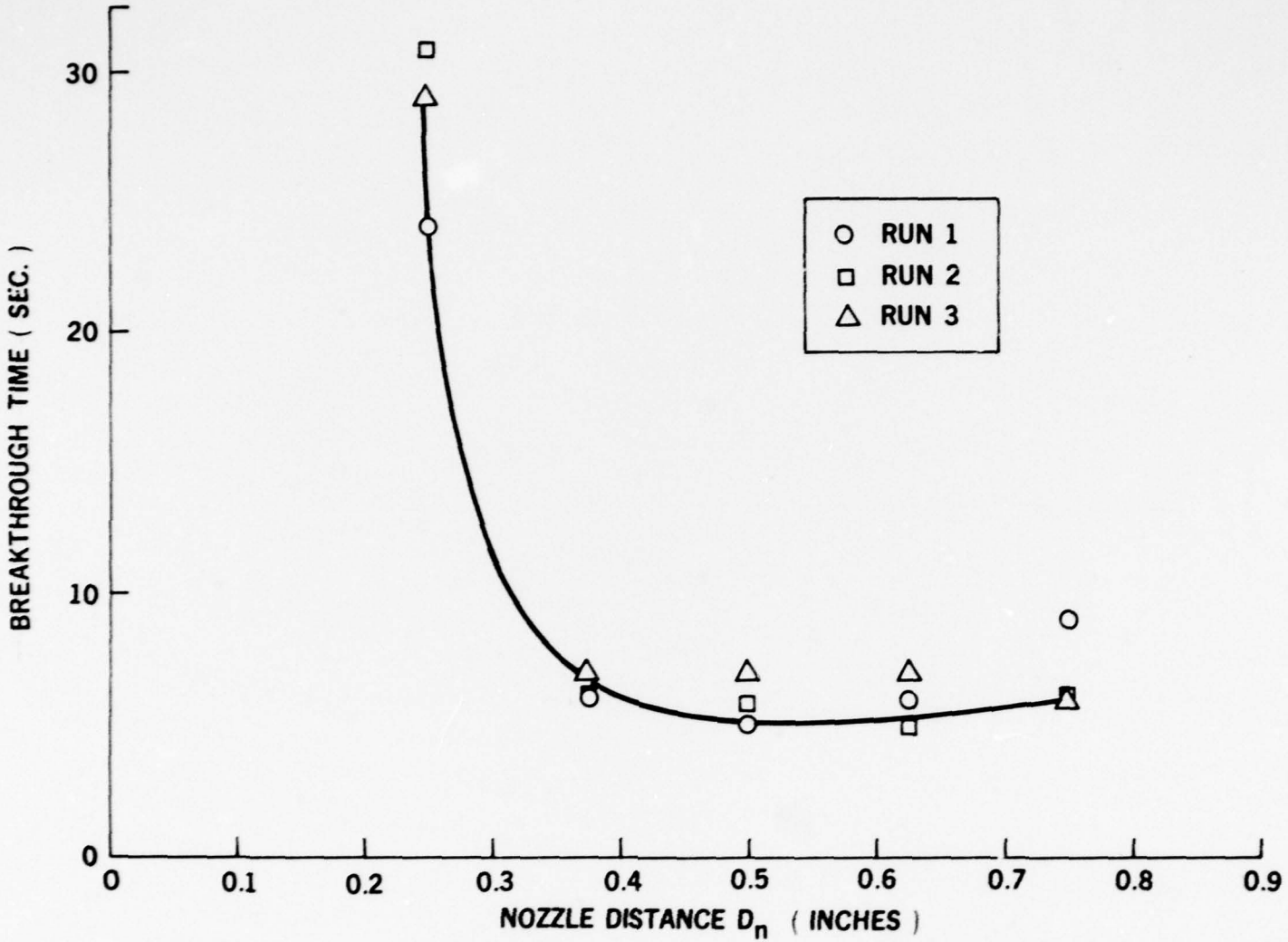

FIGURE 14 BREAKTHROUGH TIME FOR 0.030 INCH NOZZLE AS A FUNCTION OF NOZZLE DISTANCE AT 15,000 PSI NOZZLE PRESSURE

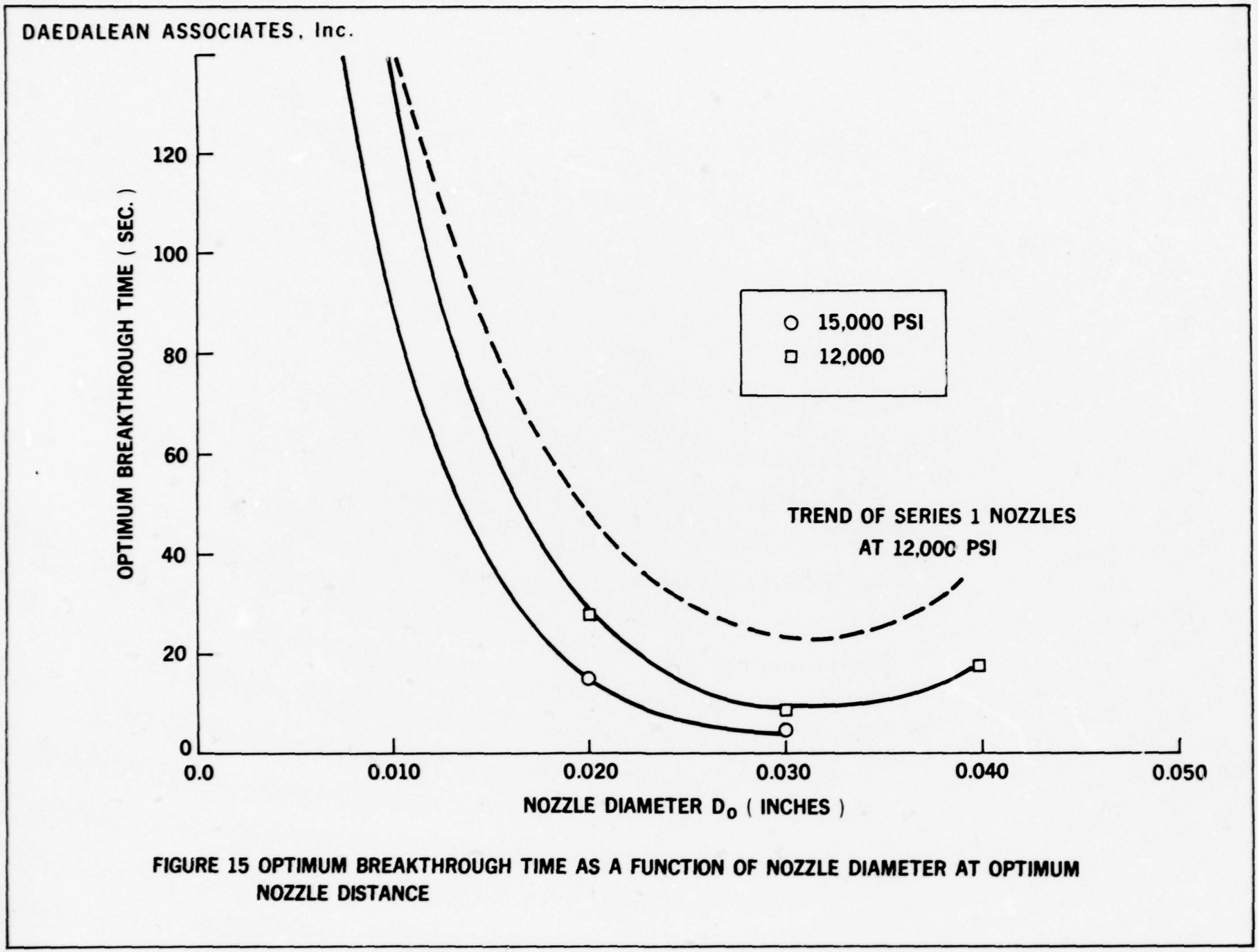

FIGURE 15 OPTIMUM BREAKTHROUGH TIME AS A FUNCTION OF NOZZLE DIAMETER AT OPTIMUM NOZZLE DISTANCE

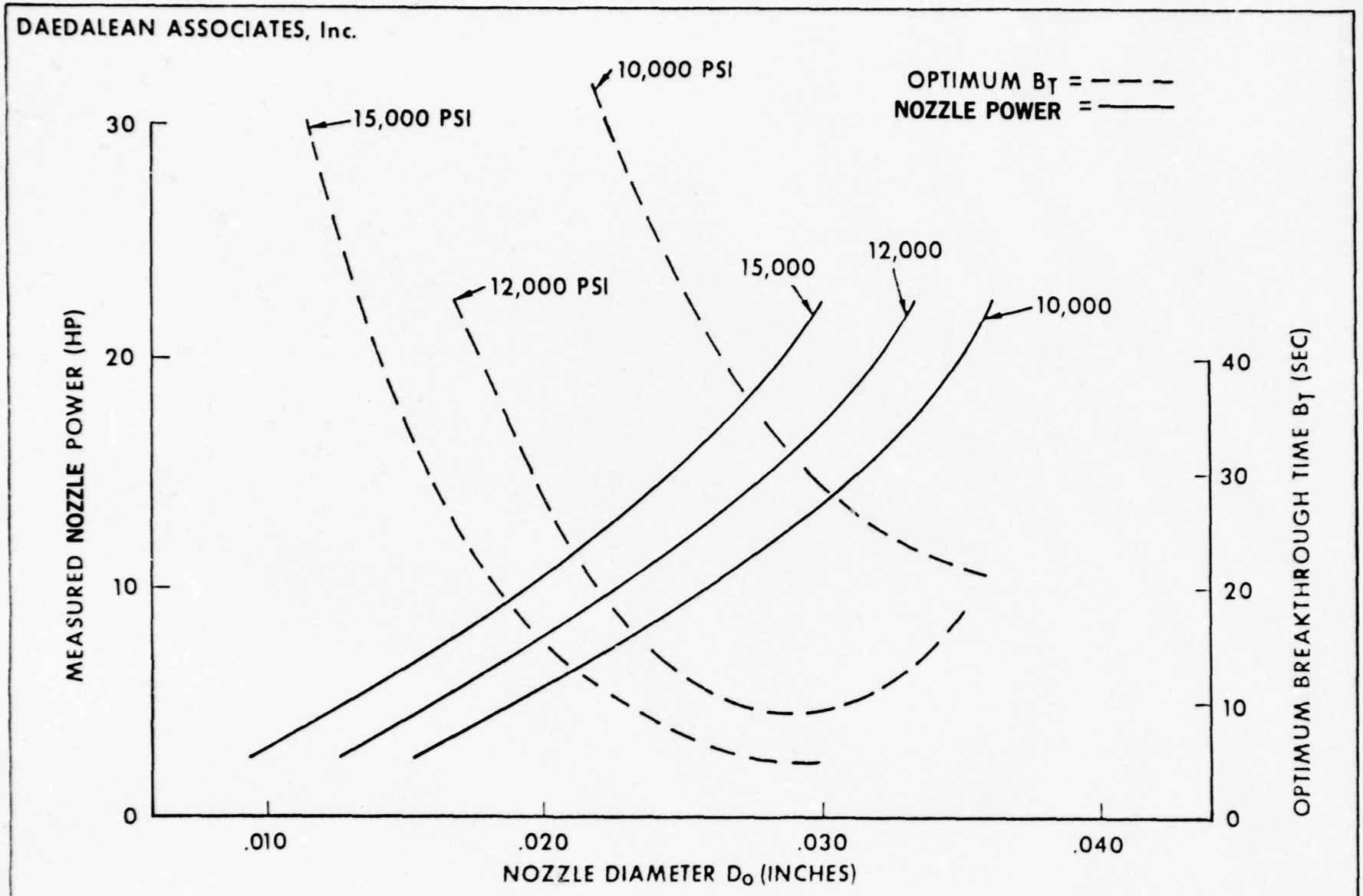

FIGURE 16 OPTIMUM BREAKTHROUGH TIME AND MEASURED NOZZLE POWER AS A FUNCTION OF NOZZLE DIAMETER AT THREE OPERATING PRESSURES

PHASE 3-A

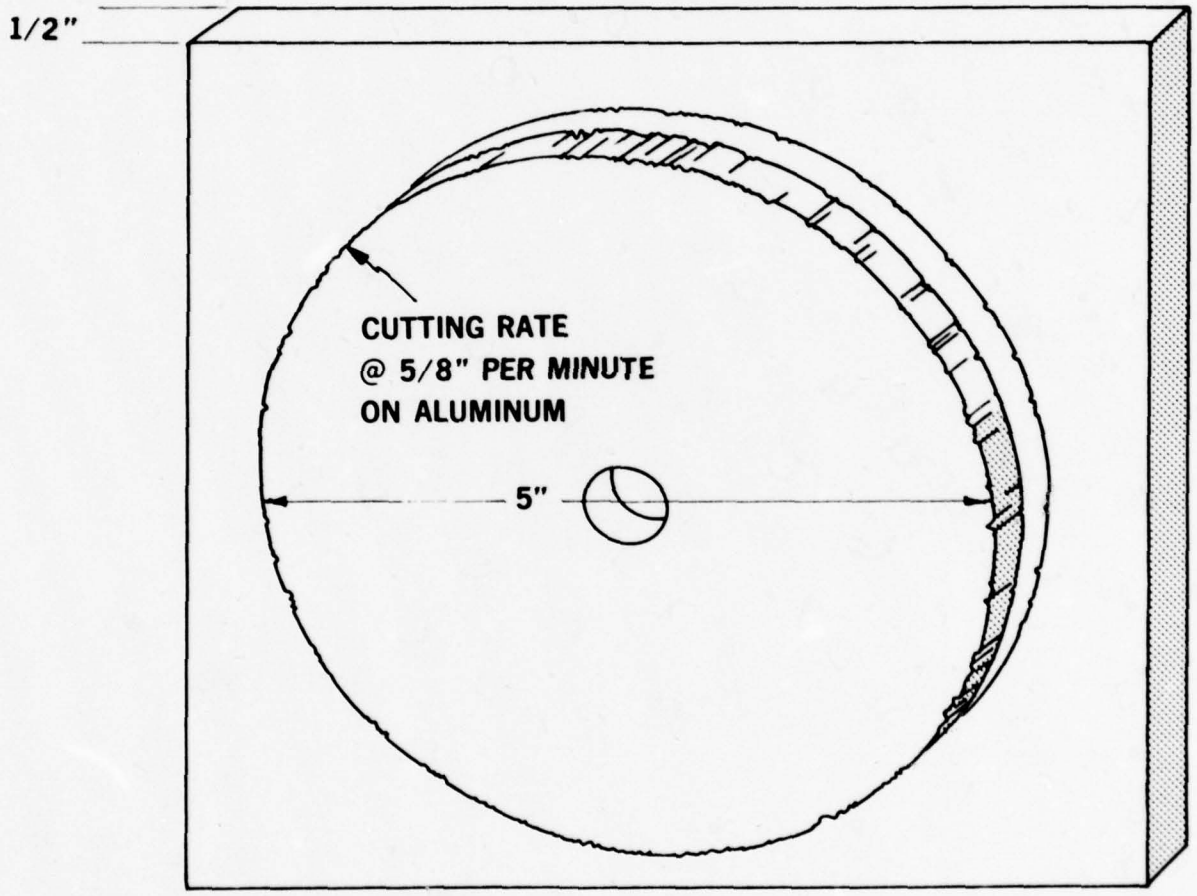

FIGURE 17 RESEARCH ON CONCAVER CUTTING TECHNIQUES FOR UNDERWATER APPLICATIONS

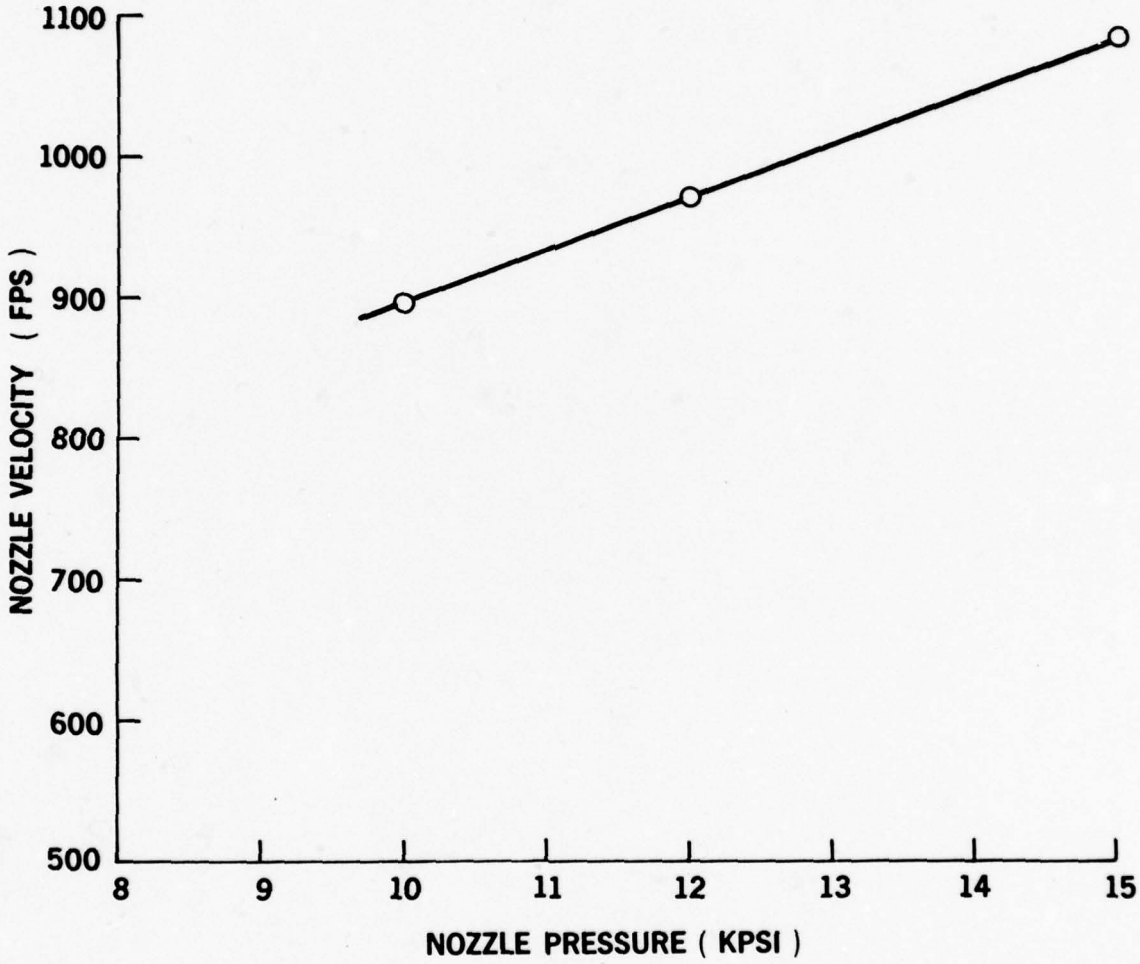

FIGURE 18 VELOCITY AS A FUNCTION OF NOZZLE PRESSURE FOR THE 0.033 INCH DIAMETER NOZZLE

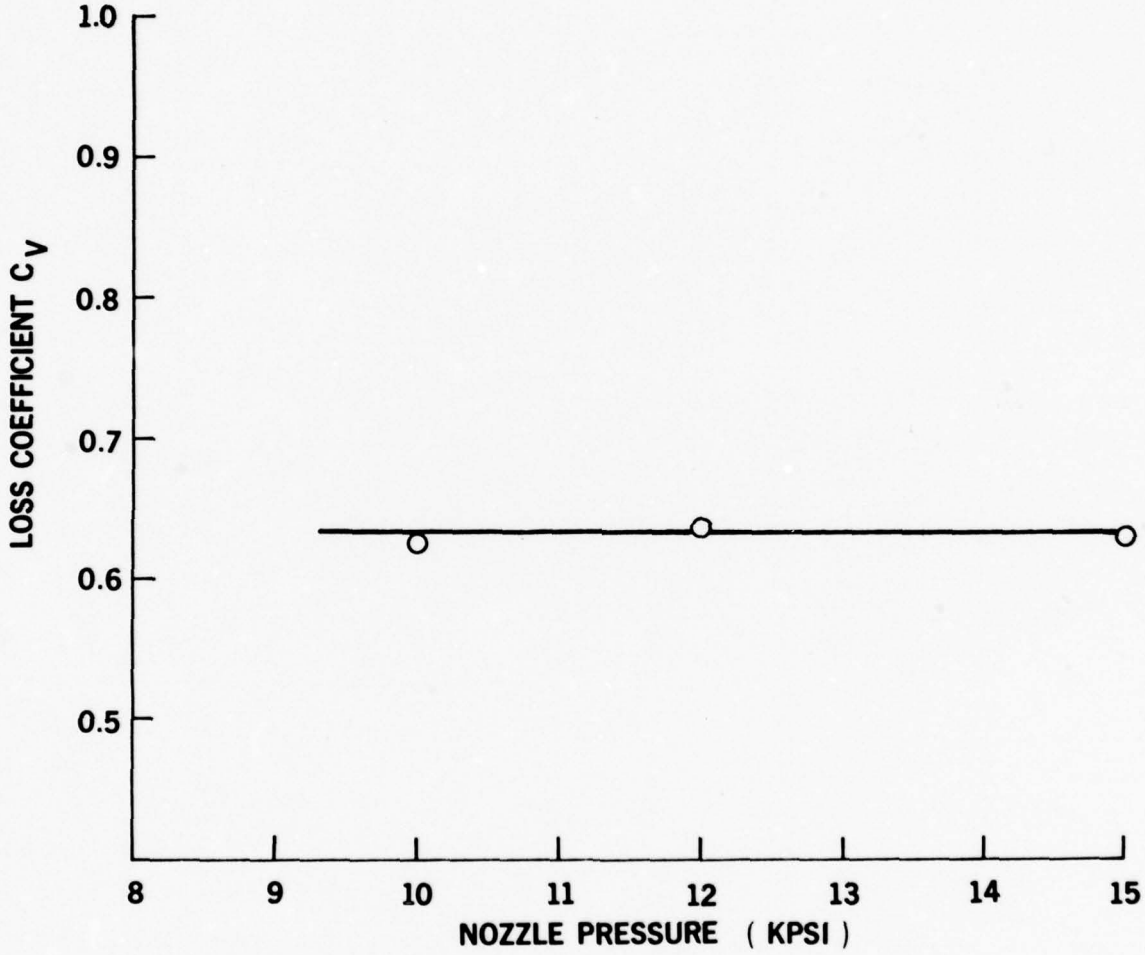

FIGURE 19 LOSS COEFFICIENT AS A FUNCTION OF NOZZLE PRESSURE FOR THE 0.033 INCH DIAMETER NOZZLE

DAEDALEAN ASSOCIATES, Inc.

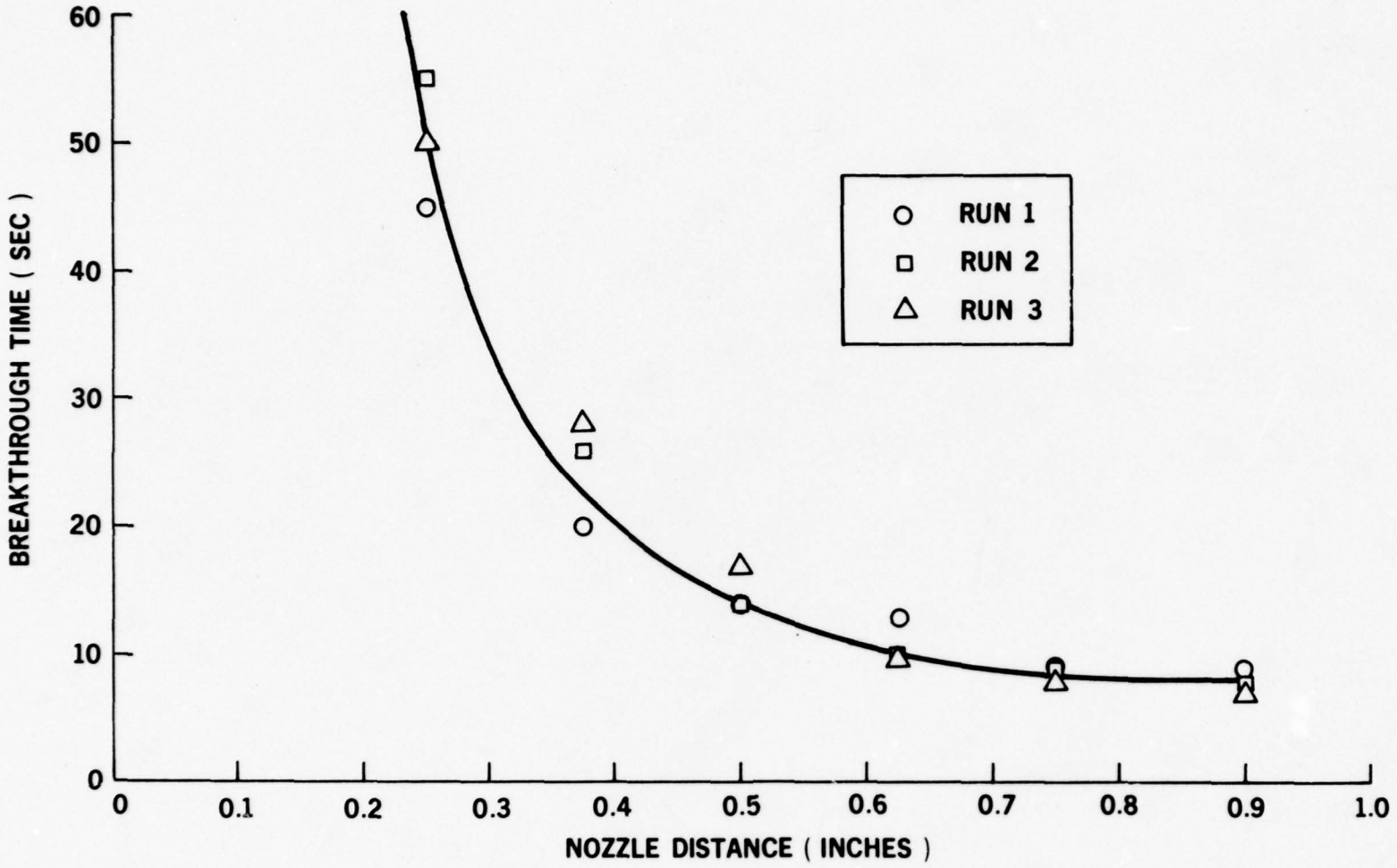

FIGURE 20 BREAKTHROUGH TIME AS A FUNCTION OF NOZZLE DISTANCE FOR THE 0.033 INCH DIAMETER NOZZLE AT 15,000 PSI NOZZLE PRESSURE

DAEDALEAN ASSOCIATES, Inc.

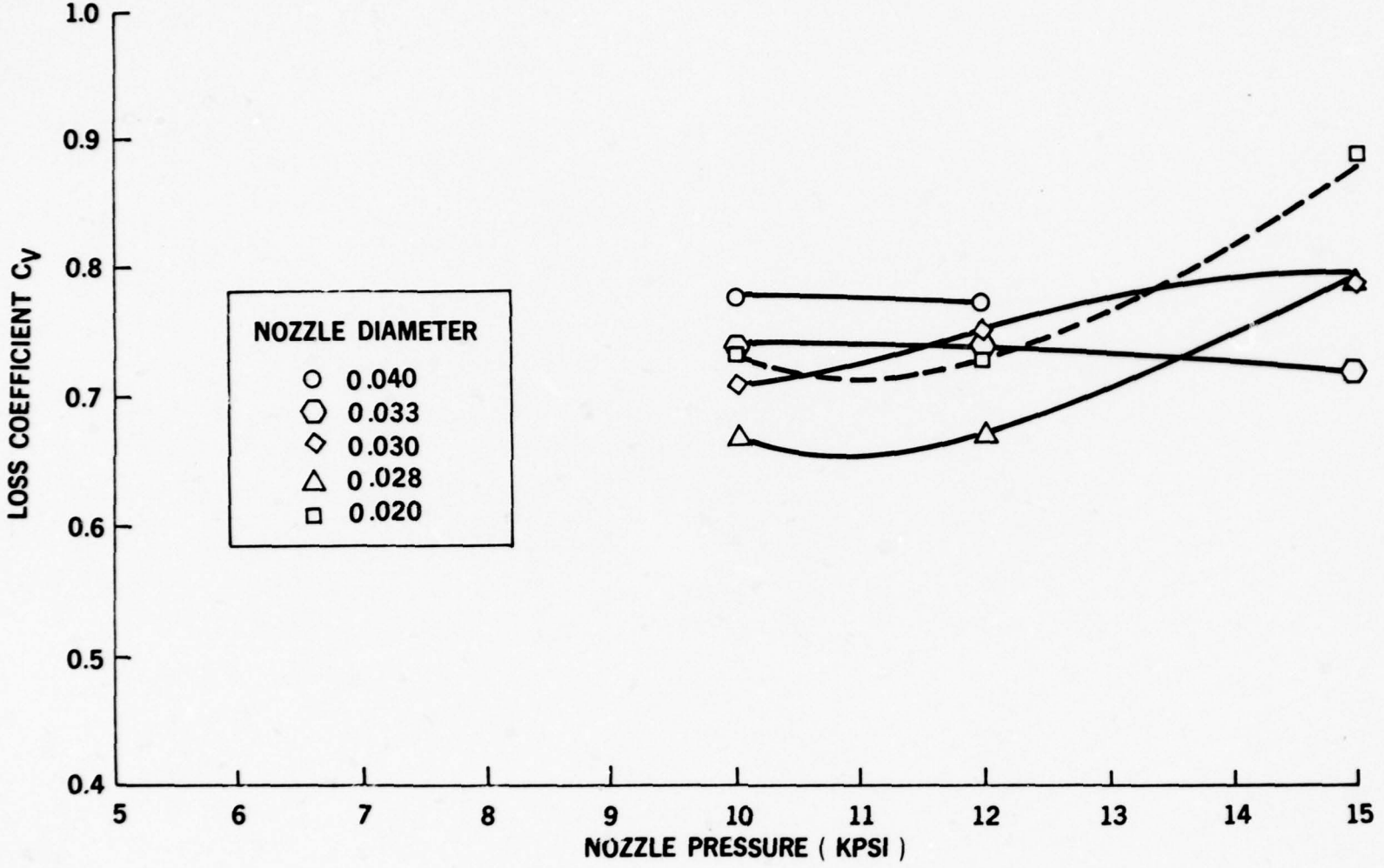

FIGURE 21 SUMMARY OF LOSS COEFFICIENT AS A FUNCTION OF NOZZLE PRESSURE

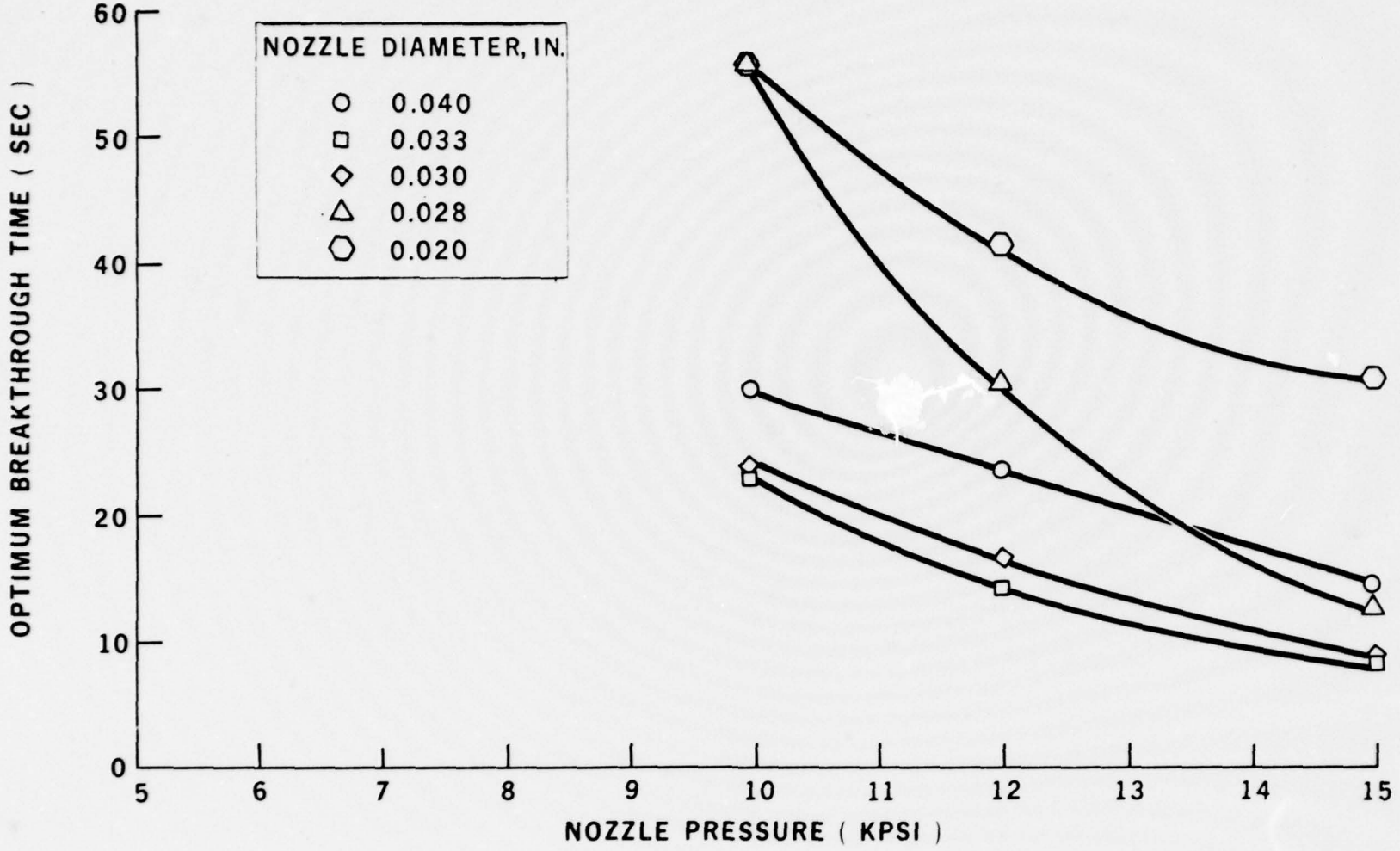

FIGURE 22 SUMMARY OF OPTIMUM BREAKTHROUGH TIME AS A FUNCTION OF NOZZLE PRESSURE FOR VARIOUS NOZZLE DIAMETERS

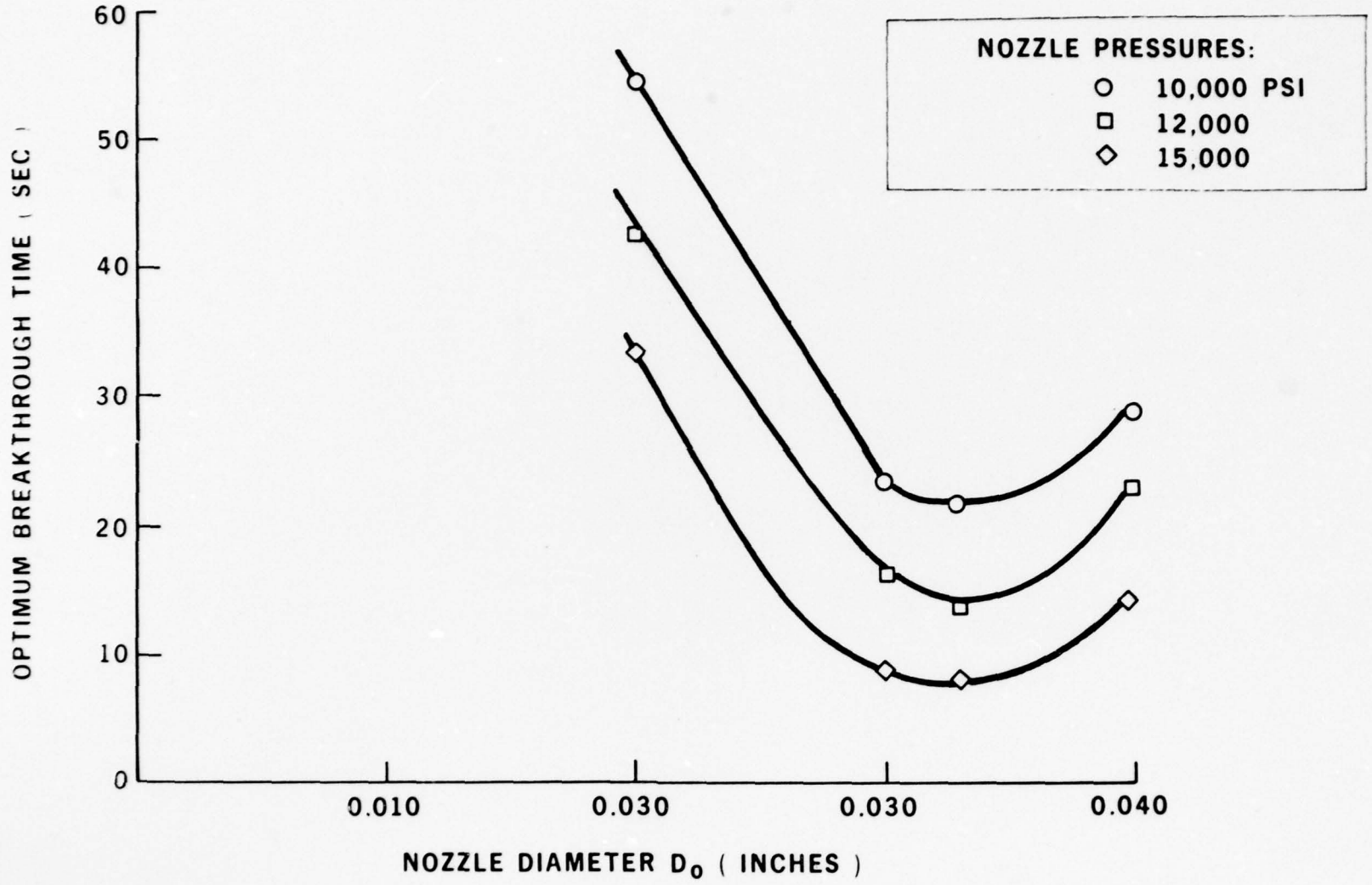

FIGURE 23 OPTIMUM BREAKTHROUGH TIME AS A FUNCTION OF NOZZLE DIAMETER AT OPTIMUM NOZZLE DISTANCE

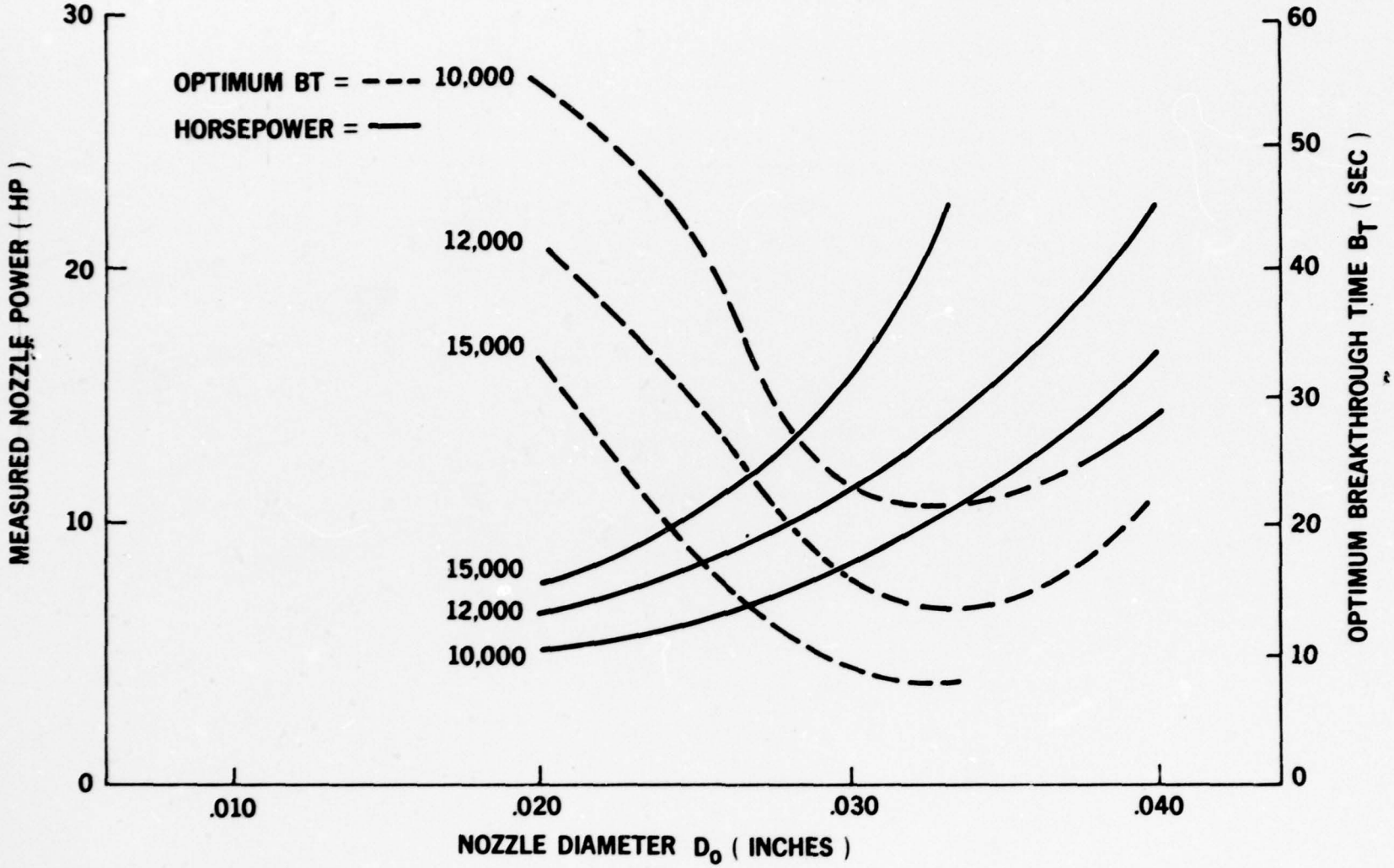

FIGURE 24 OPTIMUM BREAKTHROUGH TIME AND MEASURED NOZZLE POWER AS A FUNCTION OF NOZZLE DIAMETER FOR THREE OPERATING PRESSURES

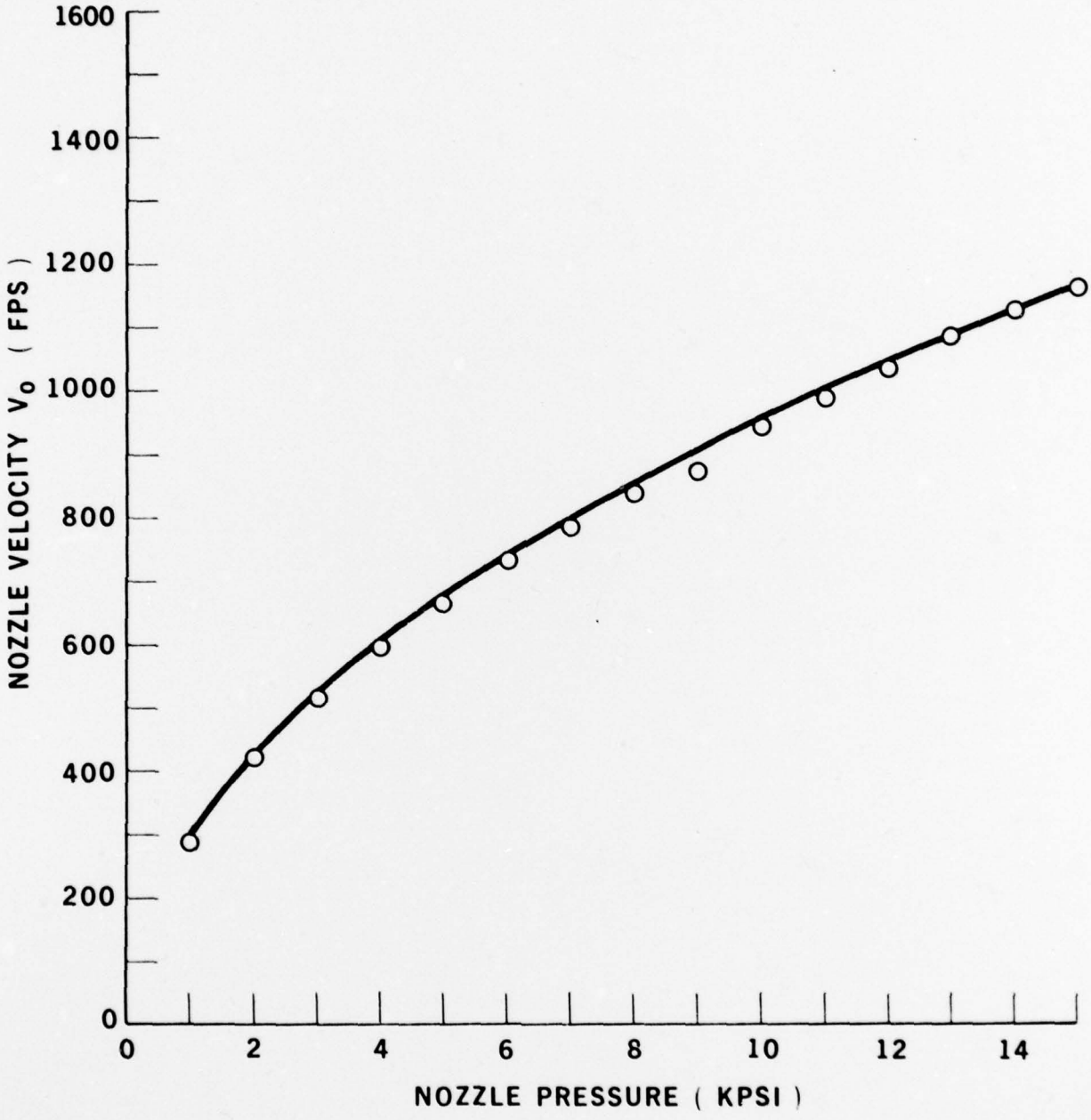

FIGURE 25 NOZZLE VELOCITY AS A FUNCTION OF NOZZLE PRESSURE FOR THE 0.040 INCH DIAMETER NOZZLE

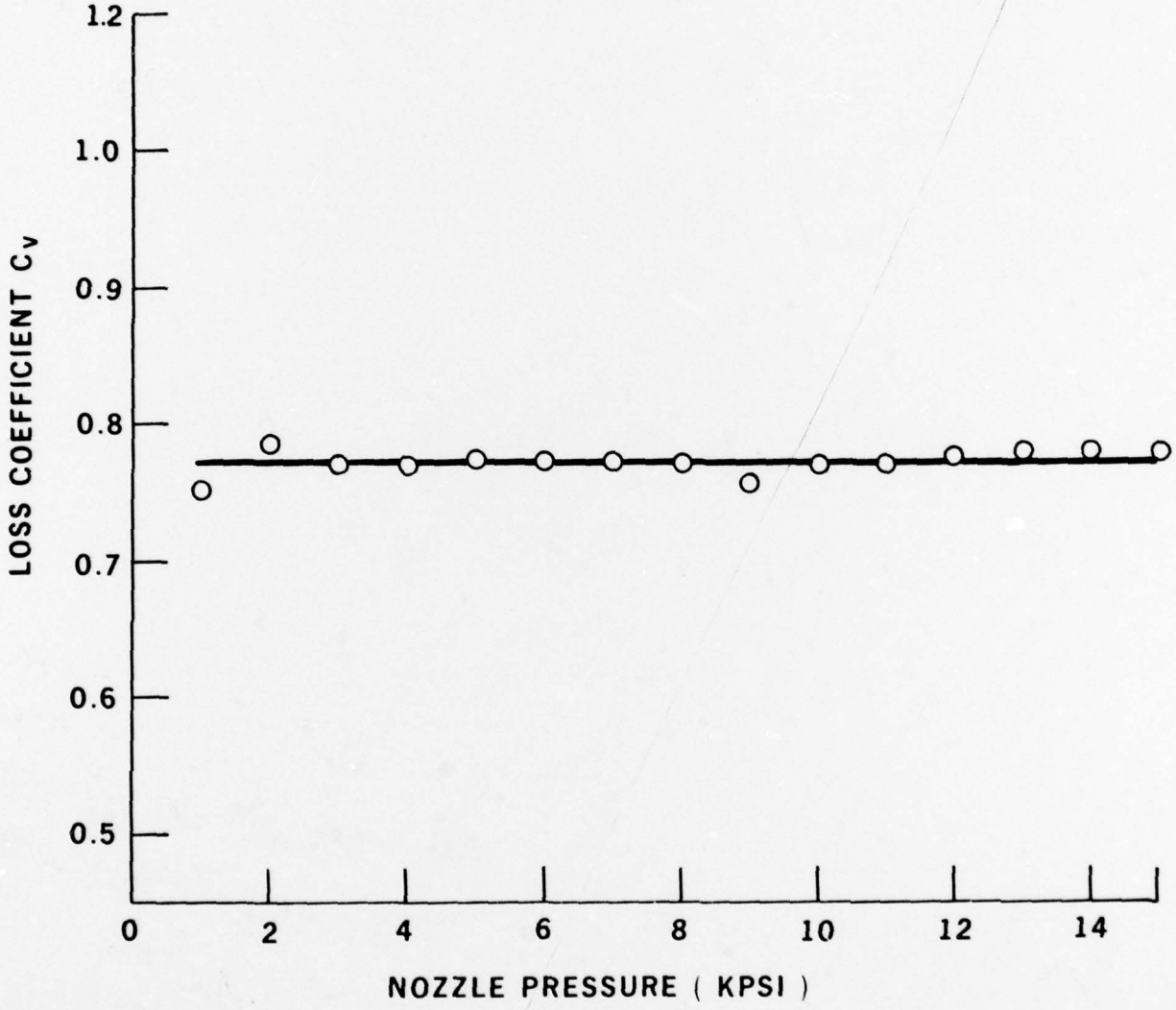

FIGURE 26 LOSS COEFFICIENT AS A FUNCTION OF NOZZLE PRESSURE FOR THE 0.040 INCH DIAMETER NOZZLE

DAEDALEAN ASSOCIATES, Inc.

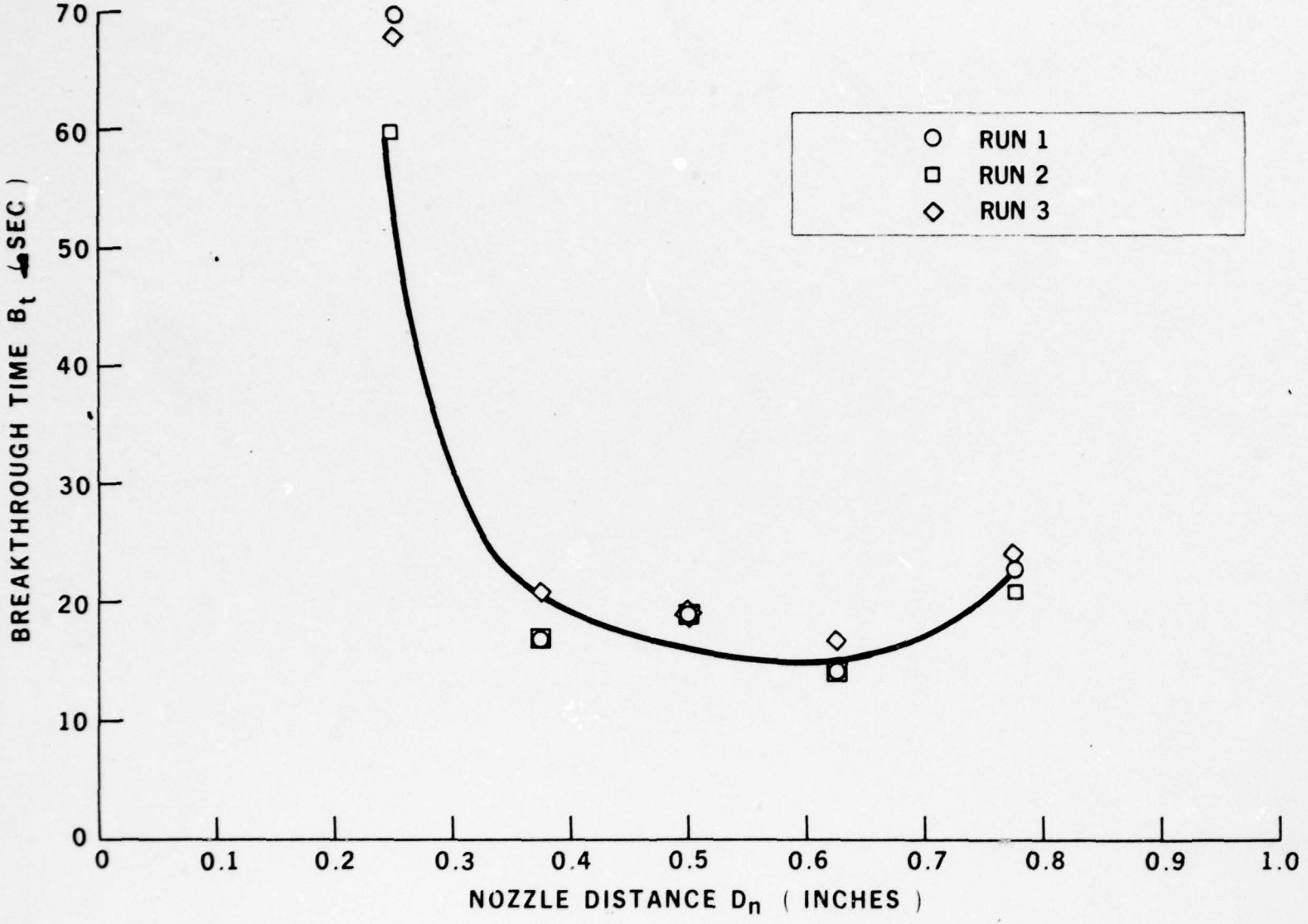

FIGURE 27 BREAKTHROUGH TIME AS A FUNCTION OF NOZZLE DISTANCE FOR THE 0.040 INCH DIAMETER NOZZLE AT 15,000 PSI NOZZLE PRESSURE

DAEDALEAN ASSOCIATES, Inc.

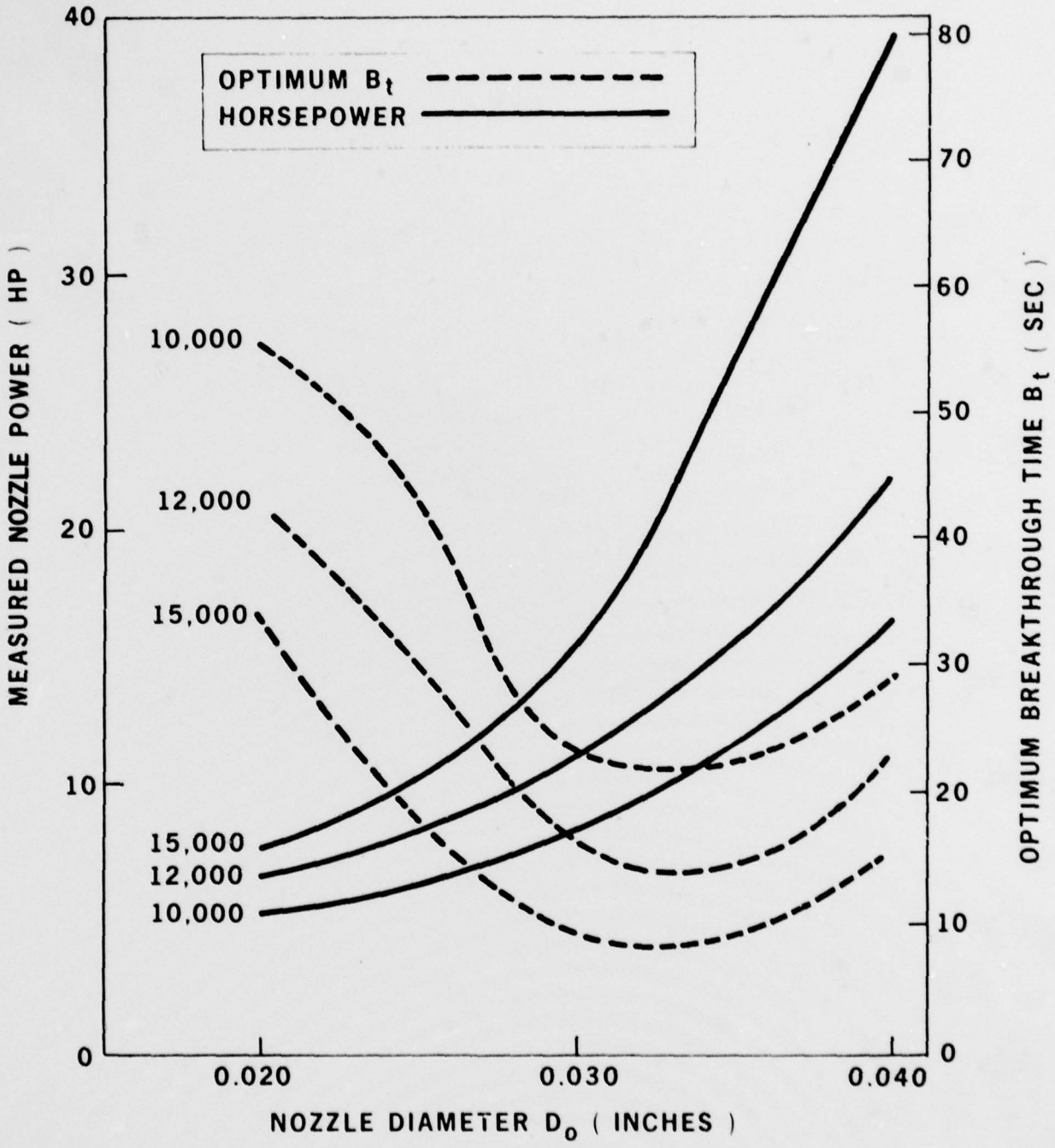

FIGURE 28 OPTIMUM BREAKTHROUGH TIME AND MEASURED NOZZLE POWER AS A FUNCTION OF NOZZLE DIAMETER FOR THREE OPERATING PRESSURES SUMMARIZED FOR THE SINGLE NOZZLES TESTED

DAEDALEAN ASSOCIATES, Inc.

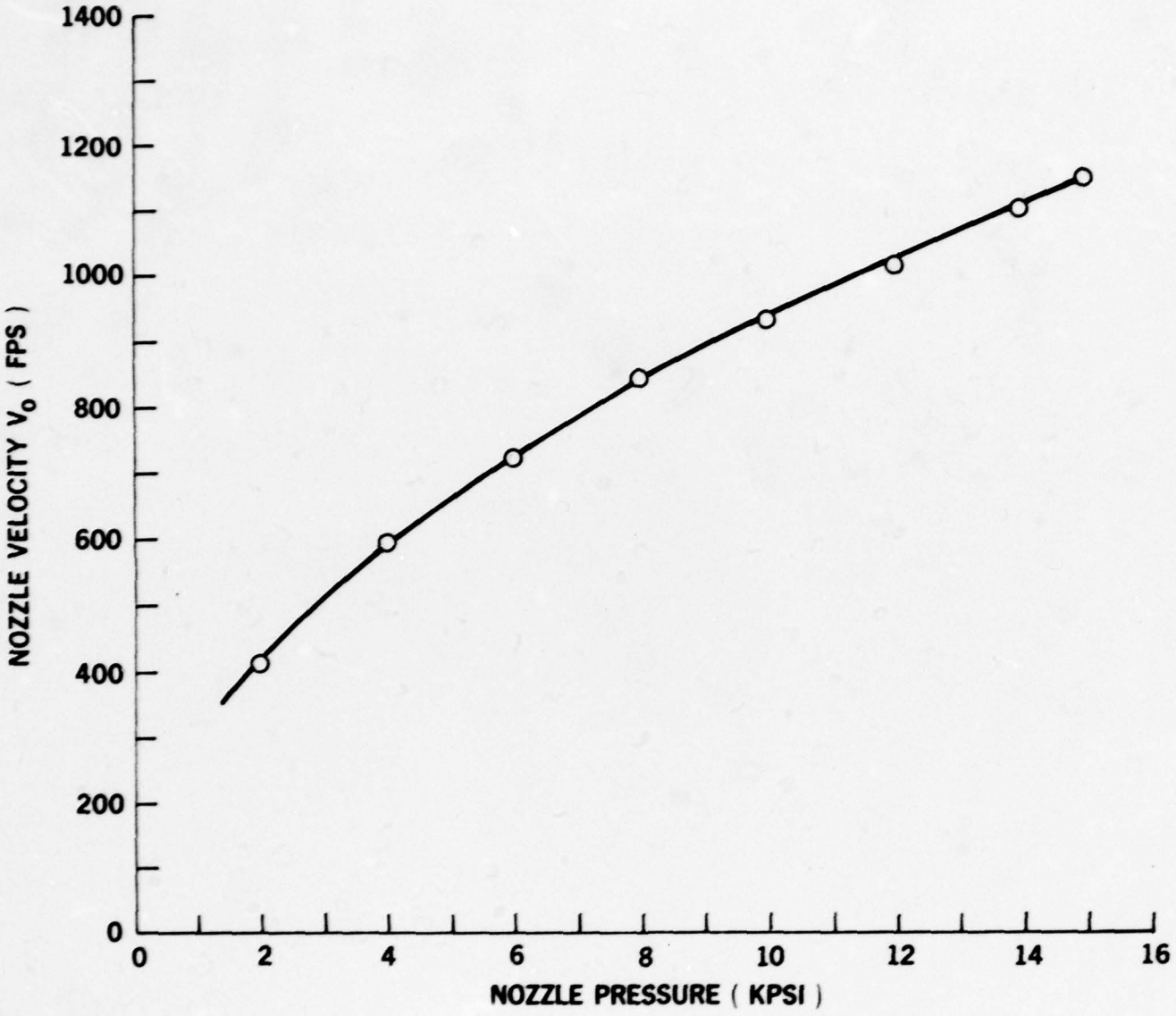

FIGURE 29 VELOCITY CALIBRATION OF TWO 0.025 INCH DIAMETER NOZZLES

DAEDALEAN ASSOCIATES, Inc

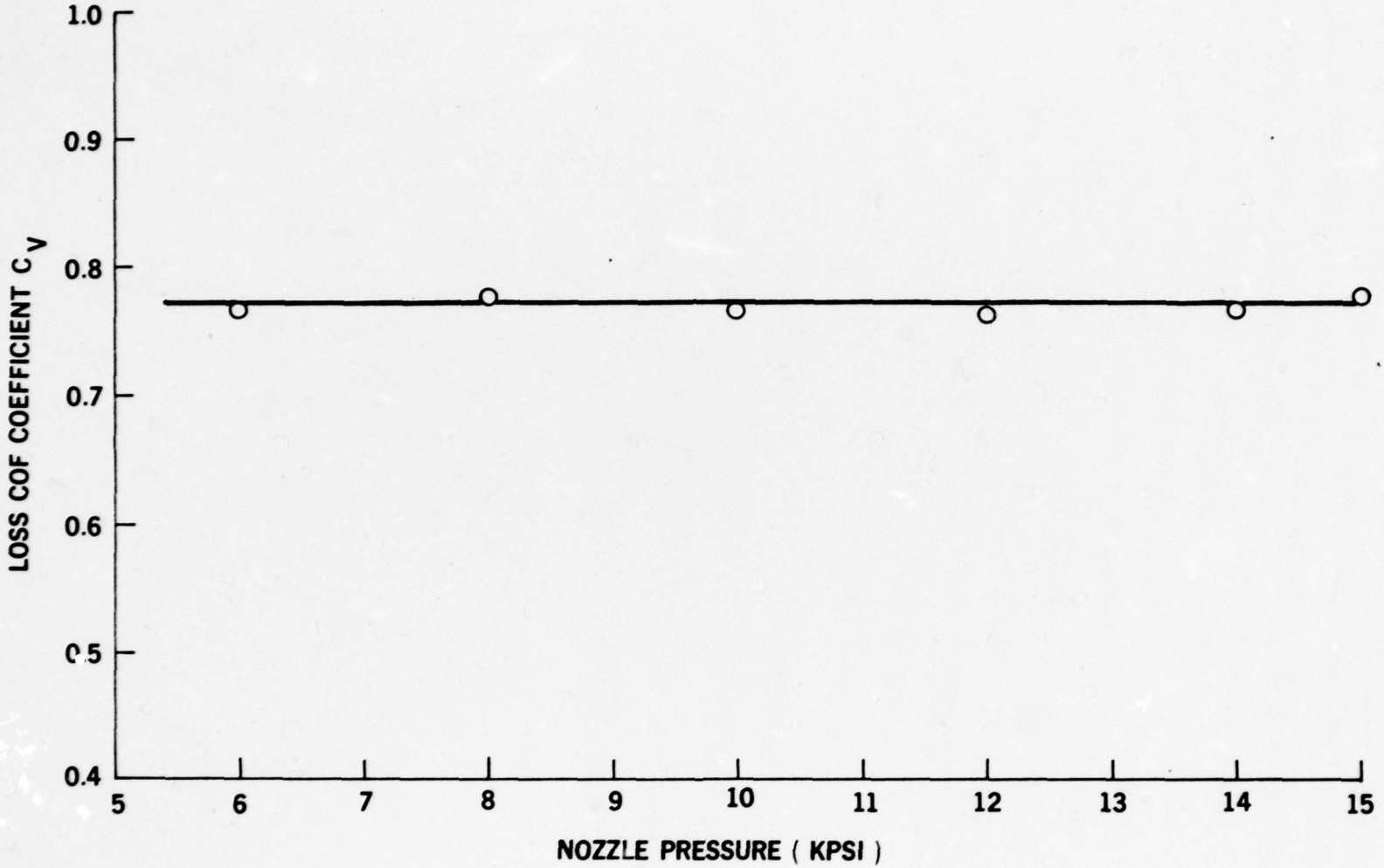

FIGURE 30 LOSS COEFFICIENT AS A FUNCTION OF NOZZLE PRESSURE FOR TWO 0.250 INCH DIAMETER NOZZLES

DAEDALEAN ASSOCIATES, Inc.

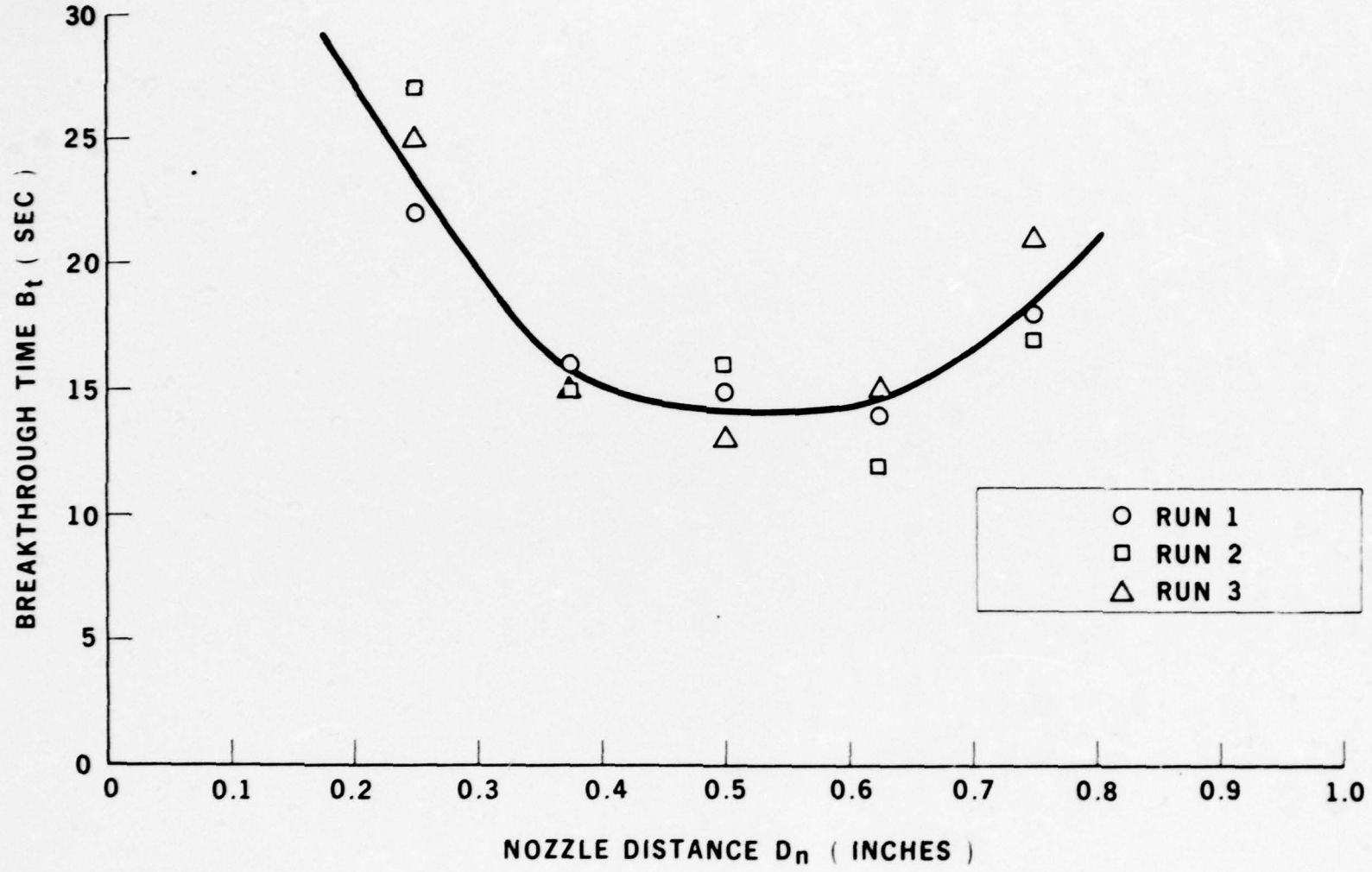

FIGURE 31 BREAKTHROUGH TIME FOR TWO 0.025 INCH DIAMETER NOZZLES AS A FUNCTION OF NOZZLE DISTANCE AT 15,000 PSI NOZZLE PRESSURE

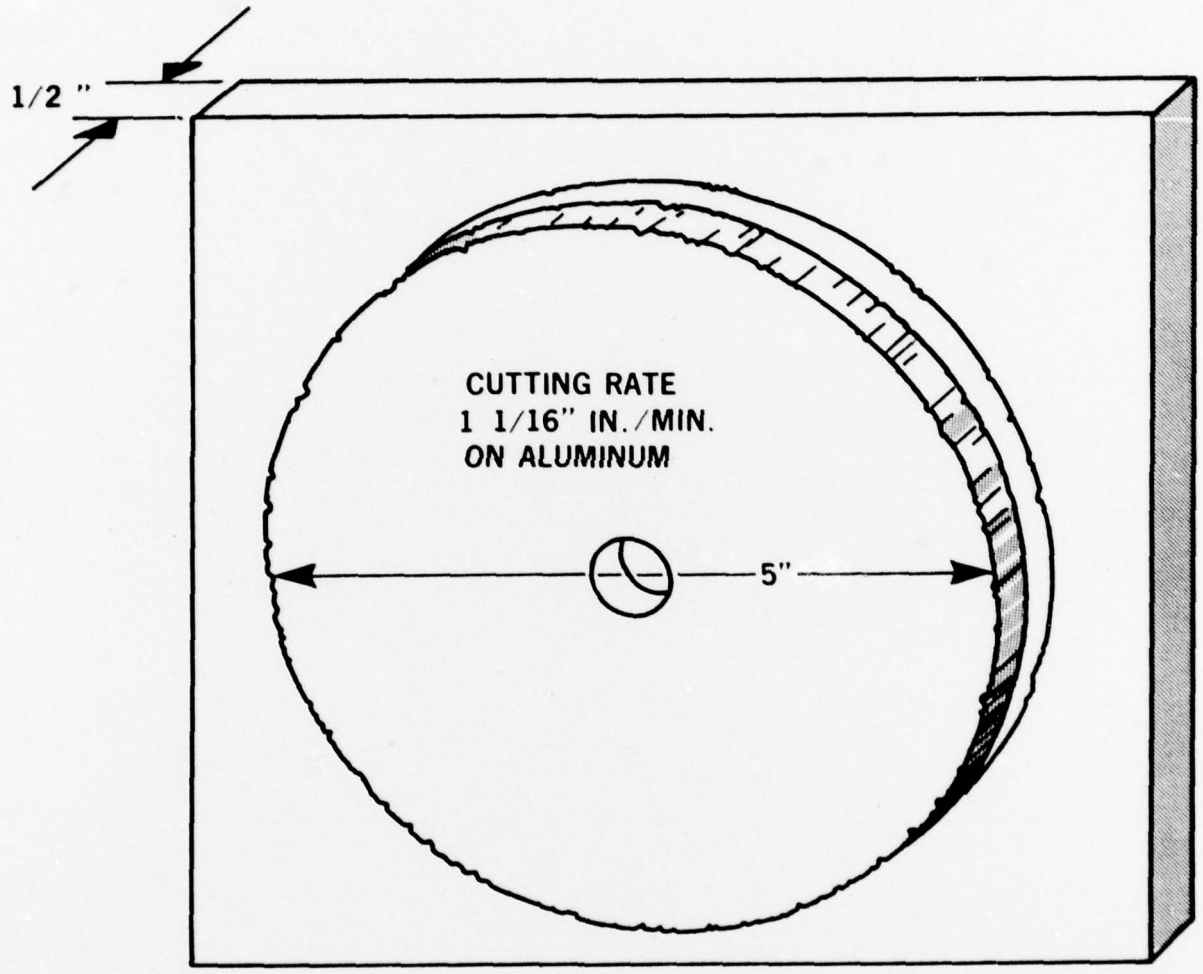

FIGURE 32 SUMMARY OF RESEARCH ON CONCAVER JET CUTTING TECHNIQUES FOR UNDERWATER APPLICATIONS

DAEDALEAN ASSOCIATES, Inc.

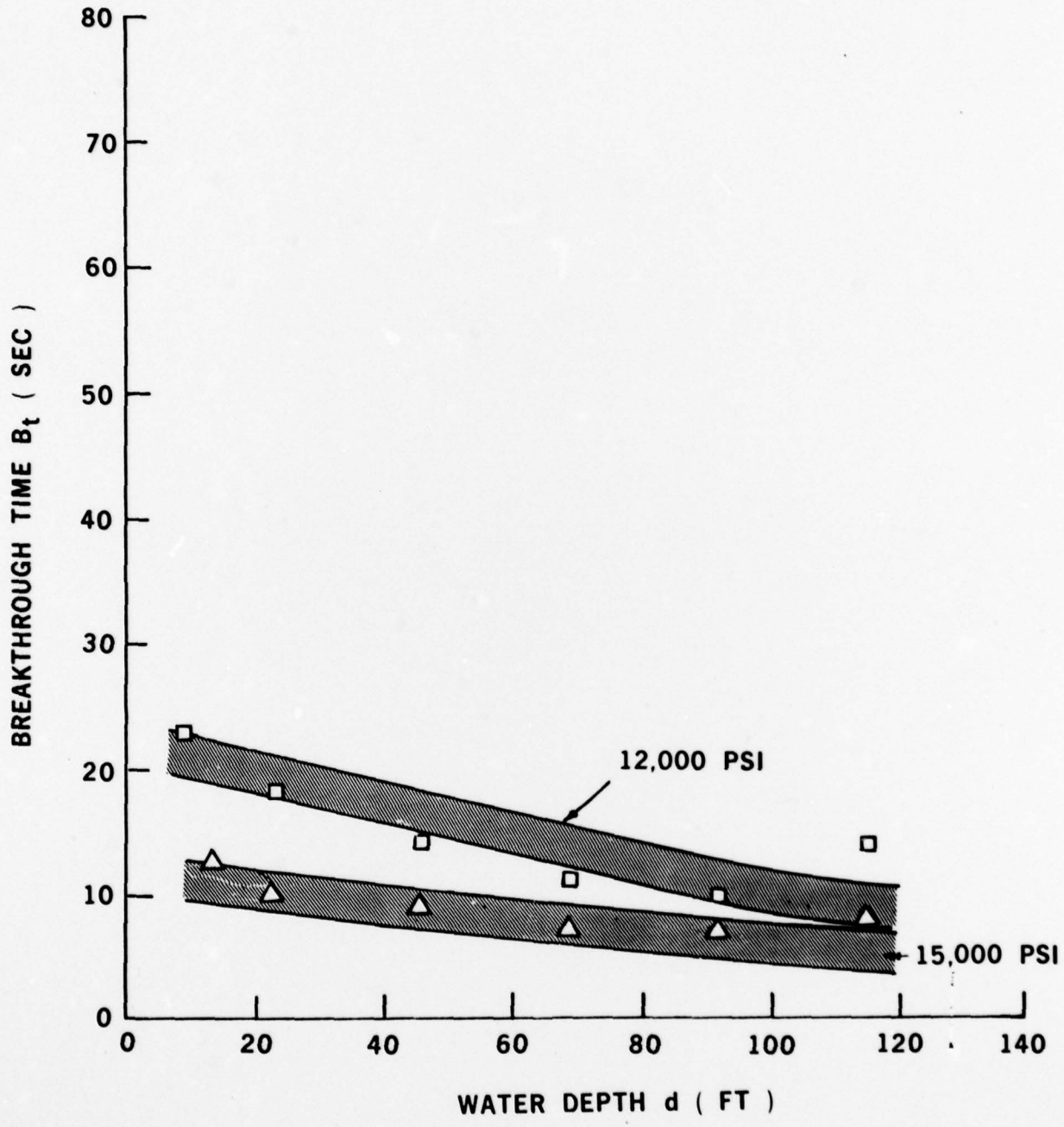

FIGURE 33 BREAKTHROUGH TIME AS A FUNCTION OF WATER DEPTH, FOR THE 0.033 INCH DIAMETER PLAIN ORIFICE NOZZLE AT OPTIMUM NOZZLE DISTANCE AND VARIOUS NOZZLE PRESSURE

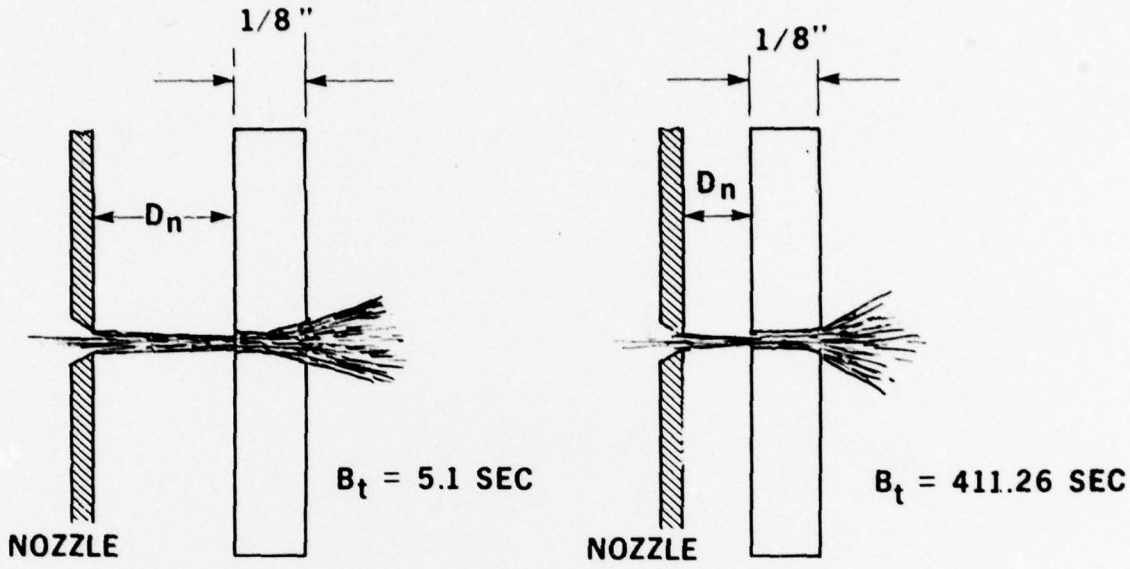

ALUMINUM

ROCKWELL NO. 15T-15

STEEL

ROCKWELL NO. 30T-56

OPTIMUM NOZZLE 0.033 INCH DIAMETER USED AT NOZZLE DISTANCE D_n OF 1/2 INCH AT 15,000 PSI

$$\frac{B_t \,|\, \text{STEEL}}{B_t \,|\, \text{ALUMINUM}} = \text{CONVERSION} = 80$$

FIGURE 34 ILLUSTRATION OF THE DEVELOPMENT OF AN ALUMINUM TO STEEL BREAKTHROUGH TIME CONVERSION

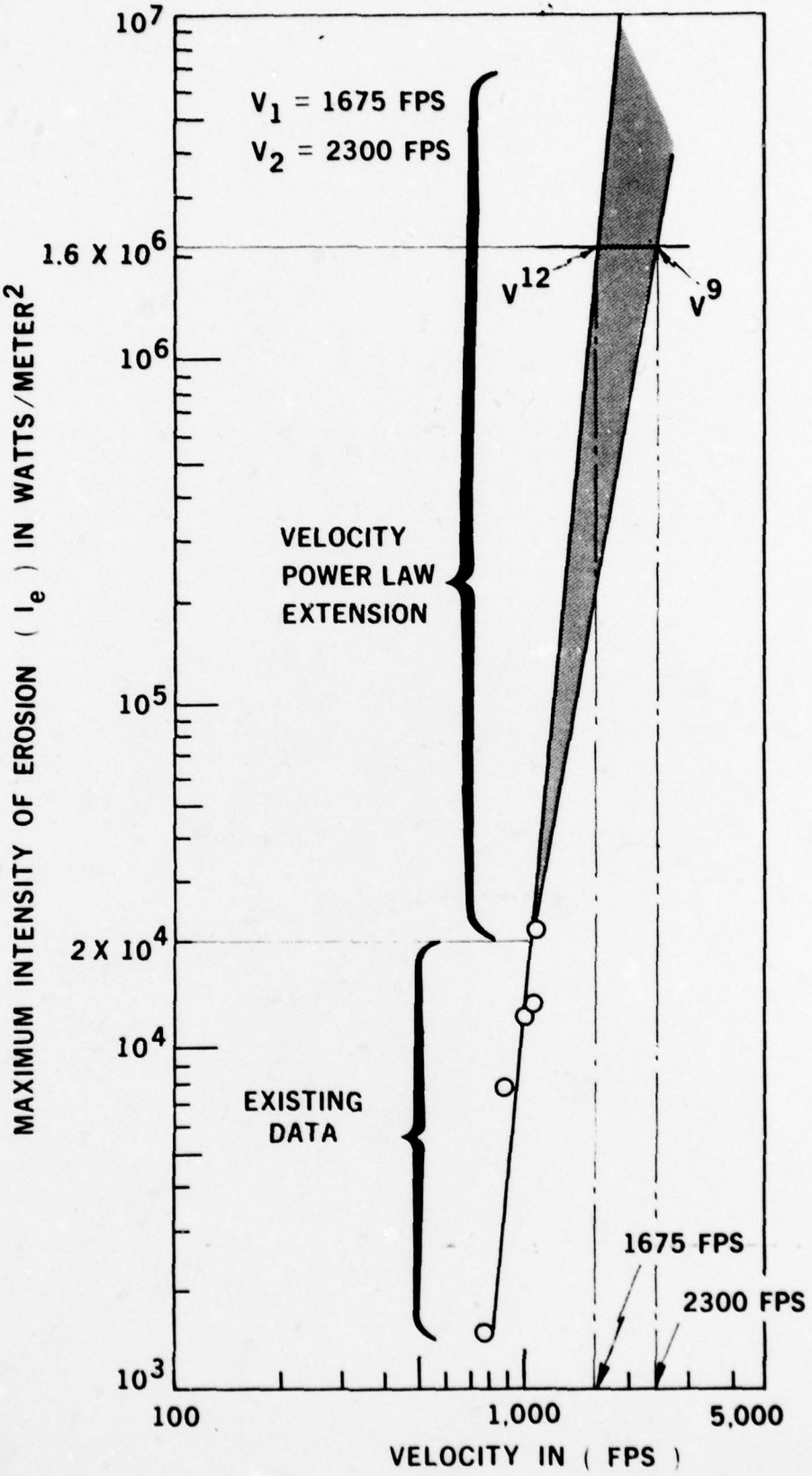

FIGURE 35 PHASE III EVALUATION OF THE POWER LAW FOR INTENSITY OF EROSION AS A FUNCTION OF NOZZLE VELOCITY - EXTENDED INTO PROJECTED OPERATING VELOCITY

SUMMARY OF ACCOMPLISHMENTS

- OPTIMIZED DIAMETER FOR SINGLE NOZZLE CUTTING
- EXAMINED AFFECT ON CUTTING RATE FOR TWO NOZZLE SYSTEM
- INITIATED CUTTING AT SIMULATED DEPTHS
- ESTABLISHED 1 1/16 IN./MIN. RATE IN 1/2" ALUMINUM
- ESTABLISHED ALUMINUM TO STEEL BREAKTHROUGH TIME CONVERSION FACTOR OF 80

FIGURE 36 SUMMARY OF TECHNICAL ACCOMPLISHMENTS FOR THE CURRENT PHASE OF THE CONCAVER CUTTING PROGRAM

FIGURE 37 - COMPARISON OF STATE-OF-TECHNOLOGY CUTTING METHODS WITH CONCAVER CUTTING SYSTEM

	Oxygen Arc	Oxygen Hydrogen	Shielded Metal Arc	Concaver System
Preheat Required		X		
Instant Start	X		X	X
Fuel Gas Required		X		
Electrodes Required	X		X	
Oxygen Required	X	X		
Cuts Ferrous Metals	X	X	X	X
Cuts Non-Ferrous Metals			X	X
Cuts Standard Thicknesses	X	X	X	X
Cuts Non-Metals		X		X
Cuts Laminated Plating	X			X
Shallow Diving Gear Permitted		X		X
Electric Shock Hazard	X		X	
Flame Adjustment Required		X		
Electrode Changing Required	X *		X	
Shipboard Explosion Hazard		X		
High Skill Required		X	X	
Usable with Small Boats		X		X
Falling Piece Danger	X	X	X	X
Special Eye Protection	X	X	X	
Continuous Cutting Process		X		X
Danger of Exploding Trapped Materials such as Gasoline, Fuel Oil, Ammunition, etc.	X	X	X	
Easily Operated in Tight Spaces	X**	X		X

*Not as frequent with ceramic electrode.
**Particularly with ceramic electrode.